Summer 1988

Molecular Study of the B19 (Human) Pathogenic Parvovirus

Jamshed Ayub
Old Dominion University

MOLECULAR STUDY OF THE B19 (HUMAN) PATHOGENIC PARVOVIRUS

by

JAMSHED AYUB

B.Sc.(Honors), 1975, Aligarh Muslim University, Aligarh, India
M.Sc., 1977, Aligarh Muslim University, Aligarh, India
M.S., 1982, Old Dominion University, Norfolk, Virginia

A Dissertation Submitted to the Faculty of Old Dominion University and Eastern Virginia Medical School in Partial Fulfillment of the Requirements for the Degree of

DOCTOR OF PHILOSOPHY

BIOMEDICAL SCIENCES

OLD DOMINION UNIVERSITY
and
EASTERN VIRGINIA MEDICAL SCHOOL
AUGUST, 1988

Approved by:

Alva H.Johnson (Director)

ABSTRACT

MOLECULAR BIOLOGY OF THE B19 (HUMAN)

PATHOGENIC PARVOVIRUS

JAMSHED AYUB

Old Dominion University, 1988

Director: Dr. Alva H. Johnson

The B19 (human) parvovirus is a small single stranded DNA virus of 5.4 kilobases. B19 is specific for erythroid progenitor cells and has been propagated in vitro only with human erythroid bone marrow. Replication of viral DNA and the viral protein products of B19 appear similar to those of other animal parvoviruses. However, B19 differs from other parvoviruses in some important aspects, which include the initiation of all transcripts at a strong left side promoter (p6) and the absence of a functional internal promoter. B19 has an unusual transcription map which is described in this study.

The transcription map of B19 suggested overlapping transcripts with the same initiation and termination sites and containing introns of differing sizes. Model experiments were performed to test the validity of two dimensional exonuclease VII analysis of overlapping transcripts. The transcripts were hybridized with a DNA probe and digested with exonuclease VII. Single bands were resolved into components of appropriate sizes by two dimensional electrophoresis.

The overlapping transcripts of B19 produce two capsid proteins, namely VP1 and VP2, where VP1 is the major protein produced. Immediately upstream from the VP1 translation site is an unusual sequence containing multiple ATG codons. During processing, this sequence is spliced out of VP2 RNA. A set of experiments were performed using synthetic RNAs to determine the role of these upstream spurious AUGs on translation. Translation of VP1 RNA was very inefficient compared to VP2 RNA in a cell free system, indicating that capsid protein production was regulated at the level of translation.

DEDICATION

Dedicated, with love, to my wife

BUSHRA SEEMA AYUB

whose love, encouragement, and persistence
helped my faltering feet, at several ocassions,
to regain control and finally finish my Ph.D. degree.

ACKNOWLEDGEMENT

This is to gratefully acknowledge the supervision and guidance of Dr. Keiya Ozawa and Dr. Neal Young in this work. This work was carried out in Dr. Young's laboratory of cell biology at the Clinical Hematology Branch of the National Institute of Heart, Lung and Blood, National Institutes of Health, Bethesda, Maryland. The author would also like to thank the members of his research guidance committee - Dr. Alva H. Johnson, Dr. Neal Young, Dr. James H. Yuan and Dr. Mark Elliott - for their guidance every step of the way and for the critical evaluation of the manuscript.

TABLE OF CONTENTS

LIST OF TABLES

LIST OF FIGURES

INTRODUCTION

The family Parvoviridae are single-stranded DNA viruses which are divided into three genera, the autonomous parvoviruses, the dependoviruses and the densoviruses (1). Members of the first two genera are viruses of vertebrates, the first being capable of autonomous replication whereas the dependo-or adeno- associated viruses (AAVs) are defective and require co-infection with a helper virus for replication. The denso-viruses are viruses of insects which are also capable of autonomous replication. The single stranded DNA is a template for its own replication with terminal hairpin loops acting as primers.

The B19 human parvovirus was discovered serendipitously in the sera of normal blood bank donors in 1975. At the time of evaluation of second generation tests for hepatitis B surface antigen (HBsAg) a number of units of donated blood were identified (2,3) which gave a line of precipitation by counter-immunoelectrophoresis (CIE) with polyvalent human sera but were negative for HBsAg by the more sensitive techniques of passive haemagglutination (PHA) and radio-immunoassay (RIA). Electron microscopy revealed a single species of virus particles with a mean diameter of 23 nm and a buoyant denstiy of 1.36-1.40 g/dl. The authors originally used the term parvovirus-like particles. Further, one of the virus-containing units of blood was designated B19. This term was used in a number of subsequent publications (4,5). Although the morphology and buoyant density of these agents suggested a parvovirus, there was at this stage no knowledge of the nature of the genetic material of these

viruses. Therefore, as papers on the diseases associated with the virus emerged, authors avoided being definitive concerning classification and the term parvovirus-like agent, PVLA(6), and serum parvovirus-like agent, SPLA(7), were used. However, recent work has permitted more definite classification of the virus. Extraction of the genome from virus found in serum of a blood donor in 1982 under annealing conditions yielded a single species of double-stranded DNA, 5.5 kilobases in length (8). Treatment with heat or alkali converted this DNA into a rapidly migrating form sensitive to the single-strand-specific nuclease S1. Under conditions of low ionic strength DNA annealing is not expected to occur. Extraction of the virus DNA under these conditions yielded DNA which co-migrated with the 5.5 kb single stranded molecule. These results indicated that the virus packages equal numbers of complementary single strands of DNA in separate virions.

Infection with this parvovirus is common (40-50% of adults are seropositive). For many years the clinical consequences of infection remained obscure. At first the virus was found in few patients suffering from non-specific febrile illness with leukopenia, but infection seemed to be wholly asymptomatic (9). In 1983, the significance of these isolated reports of rash illness became clear when an outbreak of erythema infectiosum (fifth disease) in London, England was shown to be due to parvovirus infection (10). Subsequently, such outbreaks were also found associated with B19 in Canada, Japan, the United States and Sweden. The association between human parvovirus

infection and aplastic crisis was first shown in sickle cell anemia in 1981 in both London, England and Jamaica (11,12) by reports confirming the presence of the virus in the acute phase serum specimens or showing seroconversion at the time of the crisis. It is now apparent that human parvovirus infection is responsible for more than 90% of aplastic crisis in such diverse conditions as hereditary spherocytosis, pyruvate kinase deficiency and β-thalassemia intermedia, as well as in sickle cell anemia.

Recently there has been an extensive outbreak of parvovirus in Cleveland and surrounding Cuyahoga County in the U.S.A. (13,14). In a six-month period during 1984, there were 26 cases of transient aplastic crisis and more than 450 cases of erythema infectiosum. Sera collected from cases and controls at the same time and in the same geographic area clearly showed an association between parvovirus infection and the occurrence of both transient aplastic crisis and erythema infectiosum. About one-fourth of the patients with transient aplastic crisis also had a skin rash. The disease spread among household contacts, and virus was detected in urine and throat washings of affected individuals. Viremia occurred in black patients suffering from sickle-cell disease. It occurred in white patients who had hereditary spherocytosis and later developed aplastic crisis. High concentration viremia in the patients with transient aplastic crisis was present during a limited period, from five days before to one day following the reticulocyte nadir; low-concentration viremia was detected as long as nine days after

the reticulocytye nadir. IgM antibody levels were highest at the time of the reticulocyte nadir peaking within 10 days and remaining detectable for at least three to four months. Antigen is rarely detected in patients with fifth disease. In contrast, high titers of antigen can be found in patients with hemolytic anemia and transient aplastic crisis. The reason for this discrepancy is that the symptoms in fifth disease are probably due to immune complex formation after virus has disappeared. Titers of antigen are generally higher consistent with increase in the erythroid content of bone marrow.

The sequence of events occurring in human parvovirus infection has been examined by studying infection in adult volunteers (9). Following intranasal inoculation an intense viremia developed. At the time of the viremia, virus was also detectable in the upper respiratory tract secretions, but not in urine or feces. This suggested that the virus enters by, and is shed from, the upper respiratory tract. Between 7 to 10 days after inoculation the reticulocyte disappeared and hemoglobin levels fell. These hematological changes are consistent with interruption of erythropoiesis in the bone marrow, as is seen in aplastic crisis. Lymphocyte, neutrophil, and platelet levels also showed a transient but significant drop. Infected volunteers became ill at two quite distinct times following inoculation. The first phase of illness consisted of fever accompanied by a combination of malaise, myalgia, chills, or itching. These symptoms were temporarily associated with viremia and circulating IgM/virus immune complexes. The second phase of illness started

17-18 days after inoculation. A fine, pink, maculopapular rash appeared on the limbs and/or trunk, and arthralgia and some joint swelling commenced on the following day. All these symptoms are typical of erythema infectiosum. The rash faded after 2-3 days, and the joint symptoms resolved a day or two later.

Thus we know that the same human parvovirus causes a rash illness and transient aplastic crisis. The precise pathogenesis of the rash has not yet been investigated, but it is likely to be immune mediated because it occurs after the intense viremia and at a time when a specific immune response has developed. Transient aplastic crisis, on the other hand, is a consequence of lytic infection of erythroid progenitors in the bone marrow. To date, there is no evidence of recent infection with this virus in other bone marrow failure states including aplastic anemia, transient erythroblastopenia of childhood, paroxysmal nocturnal hemaglobinuria, and adult pure red cell aplasia (15). However, parvoviruses can persist by integration of viral DNA into their host cell's genome (16). Thus, the human parvovirus remains an excellent candidate as a causative agent of chronic polyarthropathies.

Two characteristics of human parvovirus infection, the intense viremia and requirement of the virus for dividing host cells, suggest a poor fetal outlook if infection occurs during pregnancy. The virus has been shown to cross the placenta (17,18), and the frequency of parvovirus-specific IgM is significantly lower in pregnant women than in nonpregnant women of the same ages.

Until recently there has been little information about the molecular nature of the B19 virus such as replication, transcription and the resulting viral products, since B19 does not propagate in any of the cell-line cells examined. However, recent work of Ozawa and coworkers (19) report the successful propagation of B19 in tissue culture system using fresh human bone marrow cells. They obtained serum containing B19 parvovirus from a patient with sickle cell disease and transient aplastic crisis during the 1986 B19 epidemic (14). This serum was adsorbed to erythroid bone marrow mononuclear cells. The infected cells were then grown in standard growth medium in the presence of the erythroid cell-specific hormone erythropoietin. Using this culture system, they demonstrated that the replication scheme of B19 is similar to other animal parvoviruses.

Further, replication forms of B19 virus were detected in the nuclear DNA of infected bone marrow cells by Ozawa using three methods (14). The results indicated a nuclear replication site for B19 parvovirus and were consistent with the replication forms of B19 parvovirus generated by DNA polymerase in a cell-free system (26). The target and site of replication of the B19 virus appear to be an immature cell in the erythroid lineage. Specifically, B19 replicates via high molecular weight double stranded intermediates in the nucleus of infected cells.

Thus, the B19 (human) pathogenic parvovirus has a highly restricted tissue range. The molecular basis of this unusual biological behavior remains uncertain. This study tries to establish the transcription map of B19 so as to achieve some

understanding of the molecular behavior of this virus. We intend to use common molecular biology techniques such as Northern analysis, S1 analysis, RNAse protection, primer extension, functional promoter assay using CAT vector, etc.

The transcription map of B19 showed overlapping transcripts with the same initiation and termination sites but with introns of different sizes. Conventional exonuclease VII analysis using alkaline gel electrophoresis cannot discriminate among such overlapping transcripts. The protected fragments (exons plus introns of various lengths) will migrate as a single band on alkaline gel electrophoresis. We have applied a two-dimensional gel method to separate such species after exonuclease VII digestion of RNA-DNA hybrids. To test this method synthetic RNA species were prepared by in vitro transcription and a mixture of overlapping original and mutant RNAs were analyzed.

The initiation of eukaryotic translation occurs at an AUG codon. The AUG lies within a commonly occuring consensus sequence of the general form PuNNAUGN (37). From point mutation studies, the optimal sequence has been determined to be ACCAUGG (51). Spurious AUG codons upstream of the true initiation site reduce the efficiency of protein translation in laboratory constructions and in some natural systems (58-60). We noticed that the region upstream of the initiation site of the B19 VP1 gene was rich in ATG codons. We thought that this region might regulate the abundance of VP1 protein. To test this hypothesis several regions of the B19 genome were subcloned into multifunctional vectors by standard techniques (23). In vitro translation products of these

plasmids were analyzed by electrophoresis in SDS-acrylamide gels.

METHODOLOGY

The following experiments were done for establishing the transcription map B19 (human) parvovirus.

Cell Culture:

B19 parvovirus was propagated in suspension cultures of human erythroid bone marrow cells, obtained from patients with sickle cell disease after informed consent (19). Serum containing parvovirus (Minor II; 60 ug B19 RNA/ml) was incubated with the low density mononuclear cell fraction for 2 hrs at 4°C to allow adsorption in Iscove's modification of Dulbecco's medium (IMDM)(20% fetal calf serum (FCS), 0.5 u/ml recombinant erythropoietin (Amgen Biological, Thousand Oaks, CA) for 2 days at 37°C, 5% CO , 95% hunmidity). HeLa cells were cultured under similar conditions in IMDM-10% FCS.

In Situ Hybridization:

B19-infected bone marrow cells were separated into erythroid and leucocyte fractions by a panning technique using anti-leucocyte monoclonal antibodies; cytocentrifuge preparations of the erythroid fraction were fixed in 4% paraformaldehyde in phosphate buffered saline (PBS) and stored in 70% ethanol at 4°C until use. In situ hybridization was performed as described (35) by the method of Harper et al (20), except for the use of a ^{35}S-labeled nick translated pYT103 DNA probe (a full length B19 clone; 21). As samples were not denatured, hybridization with RNA and single stranded DNA were discriminated by prior treatment with RNase A (100 ug/ml for 3 hrs at 37°C) or S1 nuclease (500 u/ml for 30' at 37°C).

RNA Analysis:

RNA was prepared from control and infected bone marrow cells by guanidinium hydrochloride extraction. Polyadenylated RNA was selected on a messenger-affinity paper (Amersham, Arlington Heights, ILL; 22). Northern analysis was performed by 1.5% formaldehyde gel electrophoresis, transfer to a nylon paper (Gene Screen Plus, New England Nuclear, Boston, MASS), and hybridization with ^{32}P-pYT103 (23). For Northern analysis, samples were further treated by RNase-free DNaseI (Promega Biotec, Madison, WI) in the presence of RNasin (1 u/ul; Promega). Restriction enzyme digested fragments of pYT103 were used as molecular weight markers (undigested- 5.11 kb; Pst I digested- 3.14, 1.25, 0.72 kb; BamHl-KpnI- 3.9, 1.03, 0.18 kb). One dimensional neutral and alkaline analysis and two dimensional S1 analysis were performed by the methods of Berk and Sharp (24) and Favaloro et. al. (25), respectively. The pYT103 insert, isolated by EcoR1 digestion, was used as a probe for S1 analysis. RNA samples from cells and the pYT103 DNA probe were dissolved in 30 ul of hybridization buffer (40 mM PIPES, pH 6.4, 1 mM EDTA, 400 mM NaCl, 80% formamide). Samples were denatured at 85°C for 15' and hybridized for 3 hours at 52°C. Then it was digested with S1 nuclease (Bethesda Research Laboratories, Gaithersburg, MD) in reaction buffer (280 mM NaCl, 30 mM NaOAc, pH 4.4, 4.5 mM $Zn(OAc)_2$, 20 ug/ml denatured calf thymus DNA, 200 u/ml S1 nuclease). The digestion was for 30' at 15°C for neutral and two dimensional gels and at 37°C for alkaline gels. After agarose electrophoresis and Southern transfer, protected fragments were

detected by hybridization with nick translated ^{32}P-pYT103. Crude mapping was performed by successive rehybridization of the same filter with different ^{32}P-labeled restriction fragments from pYT103 and pYT101 (26). The filter was soaked in 0.4 N NaOH at 42°C for 30' and washed in 0.1 X SSC, 0.1% SDS, 0.2 M Tris-HCl, pH 7.5, at 42°C for 30' to remove bound labeled probes. One dimensional (alkaline) and two dimensional exonuclease VII analysis (neutral in the first direction, alkaline in the second) were similarly performed by modification of the method of Sharp et. al. (27). The DNA probes were prepared by digestion of pYT103 with Xba I or Aat II to remove the left side inverted repeat sequence (the greater part of the right side repeats are not present in pYT103). To avoid interference with enzymatic digestion by formation of a hairpin structure during hybridization, enzymatic digestion was accomplished by addition of 300 ul of reaction buffer (30 mM KCl, 10 mM Tris-HCl, pH 8.0, 10 mM EDTA, 20 u/ug single stranded DNA of exonuclease VII [Bethesda Research Laboratories]) to RNA/DNA hybrids in 30 ul of 80% formamide for 1 hr at 37°C. Protected fragments were detected by Southern analysis. Precise S1 mapping was accomplished by hybridization of RNA with radioactively end labeled probes derived from pYT103. The 5' end was labeled by T4 polynucleotide kinase after dephosphorylation with alkaline phosphatase (Boehringer-Mannheim Biochemicals, Indianapolis, IND). Strand specific 5' end labeled probes were obtained by restriction enzyme digestion, separation on agarose electrophoresis, and electroelution. Probes labeled at the 3' end

were prepared by a filling or exchange reaction with E.coli DNA polymerase I Klenow fragment or T4 DNA polymerase (Bethesda Research Laboratories); strand specific probes were produced by use of ^{32}P-deoxynucleotides selected on the basis of the sequence of the ends of the template (23). S1 protected fragments were resolved by 5% or 8% polyacrylamide-7M urea gel electrophoresis. RNase protection mapping was done according to Melton et al (28) using ^{32}P-CTP for uniform labeling of probes. Various fragments of pYT103 were subcloned into pTZ18 or 19R vectors (Pharmacia, Piscataway, NJ) and RNA probes were prepared by in vitro transcription using T7 RNA polymerase (Pharmacia). Primer extension was performed by the method of Treisman et al (29). 5'-end labeled small fragments derived from pYT103 were used as primers. RNA/DNA hybrids were dissolved in 100 ul of reaction buffer (100 mM KCl, 60 mM Tris-HCl, pH 8.3, 6 mM $MgCl_2$, 5mM dNTP, 0.8 u/ul RNasin) containing 60 u of AMV reverse transcriptase (Life Sciences Inc., St. Petersburg, FLA). Samples were incubated for 1 hour at 41°C and then extracted with phenol, chloroform, ethanol precipitated, and resolved by 5% polyacrylamideurea gel electrophoresis.

Vector Construction, Transfection and CAT Assay:

Vectors containing the chloramphenicol acetyltransferase (CAT) gene were made using a pUC9 vector (Bethesda Research Laboratories) and a CAT catridge (Pharmacia)linked to selected restriction enzyme fragments of pYT103. Frame shift mutants were made by restriction enzyme digestion of constructs followed by a filling reaction with Klenow fragment of DNA polymerase I and

recircularization by ligation (23). These constructs were introduced into HeLa cells by $CaPO_4$ transfection. They were introduced into human erythroid bone marrow cells by electroporation (30) after overnight exposure to erthropoietin. Forty-eight hrs after transfection, CAT activity was assessed by the method of Gorman et al (31). Cell lysates were incubated with ^{14}C-chloramphenicol and acetyl-CoA for 1 hr with HeLa cells and for 2 hrs with bone marrow cells. ^{14}C-chloramphenicol and its acetylated derivatives were separated by thin layer chromatography.

The following experiments were done for mapping of overlapping transcripts using two-dimensional gel exonuclease VII analysis:

Plasmid Construction:

pYT103 (a generous gift of Dr. Tattersall) is a cloned B19 (human) parvovirus genome. Various sequences of pYT103 were subcloned into a pTZ19R multifunctional plasmid vector (Pharmacia). Plasmid pTZ.BS was constructed by subcloning a pYT103 fragment extending from BglI site at nucleotide 3053 to ScaI site at nucleotide 4918. The fragment was blunted by using T4 DNA polymerase (New England Biolabs) and inserted into a HincII site of pTZ19R. The sequence from the NcoI site at nucleotide 3380 of pYT103 to the BglII site at nucleotide 3944 was removed by double restriction enzyme digestion for the construction of pTZ.NBdel. After digestion, the ends were blunted with T4 DNA polymerase, and the deleted plasmid was recircularized. Similarly, plasmid pTZ.NAdel was obtained by

deletion of the sequence between the NcoI site, at nucleotide 3380, and the AgaI site, at nucleotide 4607, from pTZ.BS. This was followed by blunting of the ends and recircularization.

In Vitro Transcription:

The three plasmids, constructed above, were linearized by digestion with XbaI restriction enzyme. They served as template for in vitro transcription reactions. Two ug of each plasmid DNA was incubated at 37°C for 90 minutes with 0.35 u/ul of T7 RNA polymerase (Pharmacia) in the presence of 0.5 mM each of ATP, CTP, GTP, and UTP in 100 ul of reaction buffer. The reaction buffer contained 40 mM Tris-HCl, pH 7.5, 6 mM $MgCl_2$, 2 mM spermidine, 10 mM NaCl, 10 mM DTT, and 1 u/ul of RNasin (Promega). DNA templates were than removed by RNase-free DNaseI (2 u/ug DNA; Promega) treatment at 37°C for 15 minutes. The transcripts were then purified by phenol-chloroform extraction and recovered by ethanol precipitation. These synthetic RNAs were given similiar names as the plasmids from which they were derived, namely BS, NBdel, and NAdel (Fig. 10).

RNA Analysis:

The size of each RNA transcript was confirmed by 1.5% formaldehyde gel electrophoresis. A 0.5 ug of RNA sample or 3 ug of RNA molecular weight marker (Bethesda Research Laboratories) were dissolved in buffer containing 2.2 M formaldehyde/50% formamide prior to electrophoresis. The gels were stained with ethidium bromide and photographed under ultraviolet light.

S1 alkaline gel analysis:

The exon size of RNA transcripts was determined by S1

alkaline gel analysis according to the method of Berk and Sharp (24). Approximately equimolar RNA samples (40 ng BS, 30 ng NBdel, 15 ng NAdel) and their mixture were dissolved with DNA probe in 30 ul of hybridization buffer (40 mM PIPES, pH 6.4, 1 mM EDTA, 400 mM NaCl, 80% formamide). The DNA probe was 0.5 ug plasmid pTZ.BS DNA linearized by EcoRI digestion. Hybridization was carried out at 52°C for 3-4 hours. Then samples were digested with S1 nuclease at 37°C for 30 minutes by adding 300 ul of reaction buffer, which contained 280 mM NaCl, 30 mM NaOAc, pH 4.4, 4.5 mM $Zn(OAc)_2$, 20 ug/ml calf thymus DNA, 200 u/ml S1 nuclease (Bethesda Research Laboratories). Protected fragments were resolved by 1.5% alkaline agarose gel electrophoresis, Southern transfer to Gene Screen Plus nylon membrane (New England Nuclear), and hybridization with nick-translated ^{32}P-pYT103. Restriction enzyme fragments of pYT103 were used as molecular weight markers.

Exonuclease VII analysis:

One dimensional alkaline gel exonuclease VII analysis was performed by the method of Sharp et al (27). RNA-DNA hybrids were digested with exonuclease VII at 37°C for one hour by adding 300 ul of reaction buffer. The reaction buffer consisted of 30 mM KCl, 10 mM Tris-HCl, pH 8.0, 10 mM EDTA, 1 mM DTT, 10 u/ug single stranded DNA of exonuclease VII (Bethesda Research Laboratories). Protected fragments were detected by Southern analysis as described above. Exonuclease VII protected RNA-DNA hybrids also were analyzed in neutral agarose gel followed by Southern transfer. Two-dimensional gel analysis (neutral in the first

direction, alkaline in the second) was similarly performed as two dimensional S1 analysis.

The following experiments were done to determine the regulation of capsid protein translation:

Plasmid constructions:

pYT103c is a corrected version of the full length B19 genome clone pYT103. Various regions of pYT103c were subcloned into multifunctional vectors pTZ18R or pTZ19R by standard techniques (23, Fig. 14A,B). These are

1. pTZ.SR - A fragment extending from the SmaI site, at map unit 38, to the EcoRI site, at map unit 95, was subcloned into the HindIII (blunted)-EcoRI sites of the pTZ19R vector.
2. pTZ.TR - Constructed from the Tth111I (blunted)-EcoRI fragment (map unit 42-95) by similiar subcloning into pTZ19R.
3. pTZ.SR(THdel) - Constructed from pTZ.SR by digestion with Tth111I and HindIII to remove the region between map units 42-45, followed by blunt ending and recircularization.
4. pTZ.SR(Hmu) - Constructed from pTZ.SR by HindIII digestion, followed by blunting and recircularization.
5. pTZ.HR - Constructed from the HindIII-EcoRI fragment (map units 45-95) by subcloning into pTZ19R between the HindIII and EcoRI sites. However, the distance between the cap site and translational initiation site was less than 20 nucleotides which was too short for in vitro translation to occur. The same region was transferred into pTZ18R at the HindIII site in order to increase the distance between the cap and the initiation sites by

adding multiple cloning sites upstream. An ATG codon at the SphI site within this area of multiple cloning sites of pTZ18R was removed prior to cloning. This was done by SphI digestion followed by mung bean nuclease digestion of the protruding nucleotides. The pTZ18R was then recircularized by ligation.

6. pTZ.BR - Constructed from the BglI-EcoRI, map units 57-95, fragment of pYT103c. The BglI site was blunt ended and ligated to a HindIII linker prior to insertion into the vector at the HindIII-EcoRI sites of pTZ19R.

7. pTZ.SHBR - Constructed by digesting pTZ.SR with HindIII and EcoRI, which removed the VPI coding and other 3′ sequences and left only the upstream noncoding region,and subcloning of the BR fragment, map units 57-95, from pTZ.BR downstream. In this construct, both the last minicistron and the coding region of VP2 were in the same reading frame (50). To obtain an authentic VP2 translation product, the reading frame of the upstream regions was altered by a frame shift mutation at the HindIII site within the last minicistron. For reading frame 3, namely SH.BR(3), it was altered by HindIII digestion followed by filling with Klenow fragment of DNA polymeraseI and recircularization. SH.BR(2), reading frame 2, was altered by HindIII digestion followed by removal of 5′ extensions with mung bean nuclease and recircularization.

In Vitro Transcription:

Linearized pTZ plasmids containing the various pYT103c fragments were transcribed in vitro by T7 RNA polymerase in the presence of the cap analogue $m^7G(5')ppp(5')G$ to obtain large

quantities of capped RNA following the manufacturer's protocol (Pharmacia). DNA templates were removed by DNaseI digestion, followed by phenol extraction and ethanol precipitation. Production of full length transcripts was confirmed by formaldehyde gel electrophoresis.

In Vitro Translation:

50 ng of each of the in vitro transcripts were translated by rabbit reticulocyte lysate in the presence of ^{35}S-methionine (1200 Ci/mmol) for 20 or 60 minutes at 30°C according to the manufacturer's instructions (Promega Biotec). One fifth of the reaction mixture was analyzed by electrophoresis in 8% SDS-polyacrylamide gels. To detect B19 specific proteins, immunoprecipitation was performed using a specific convalescent phase serum.

The following experiments were done to study parvovirus cytotoxicity:

Plasmid Construction:

Single plasmids were constructed containing both the gene encoding for neomycin phosphotransferase under the regulation of SV40 promoter (neo^r) and either an almost full length copy of B19 genomic DNA or the left side of the B19 genome extending from map unit 0-58.

In Vitro Transfection:

Hela cells were transfected with linearized single plasmids and selected in the presence of the antibiotic G418 for 12 days. The transfection of HeLa cells ($1.5X10^5$ cells/100 mm dish) was

done by calcium phosphate coprecipitation with 7.5 ug of supercoiled plasmid (exp 1, Table 1) or 1 ug and 4 ug (exp 2 and 3 respectively, Table 1) of linearized plasmids. The total DNA amount in each transfection was adjusted to 30 ug (exp 1) or 20 ug (exp 2 and 3) / dish with carrier DNA (pUC9, pUC19, or calf thymus DNA). Controls contained carrier DNA only. Two days after transfection, medium containing G418 (500 ug/ml) was added. The number of G418 resistant colonies was determined 12 days after transfection.

TABLE I

INHIBITION OF TRANSFORMATION BY SINGLE PLASMIDS CONTAINING BOTH B19 AND NEO^R SEQUENCES

PLASMID	NUMBER OF G418 RESISTANT COLONIES/DISH		
	exp 1	exp 2	exp 3
Control	0	0	0
pSV2neo	182	433	119
pB19SVneo	ND	21	7
pB19XmuSVneo	ND	448	102
pNSSVneo	2	28	13
pNSmuSVneo	138	266	90

ND = NOT DONE

RESULTS

TRANSCRIPTION MAP

RNA was extracted from B19 parvovirus infected human erythroid bone marrow cells. A Northern analysis (Fig. 1) of this RNA, using a B19 specific probe, revealed three major bands of 3.3, 2.4, and 1.0 kb. Multiple RNA species were resolved using S1 analysis, employing a full length B19 probe (pYT103 insert DNA), in neutral and alkaline gels (24). The neutral gels allowed the determination of transcript length while the alkaline gels helped determine exon length. Five transcripts - 3.1, 2.3, 2.2, 0.8, and 0.65 kb - were seen in neutral gels (Fig. 2A). In the alkaline gel the 2.2kb band was replaced by two new bands of 1.95 and 0.3 kb (Fig. 2B). This indicated the presence of at least one spliced species.

Two dimensional S1 analysis distinguished spliced and unspliced RNA transcripts by separating by size in the first, neutral dimension and further separation into exons in the second, alkaline dimension. This method revealed eight transcripts (Fig. 2C), of which four RNA were spliced: c composed of exons of 0.3 and 1.95 kb; d of 0.2 and 1.95 kb; g of 0.3 and 0.3 kb; and h of 0.2 and 0.3 kb exons. The other four RNA species, namely a, b, e, and f, lay along the diagonal of the two dimensional gel, where e and f were slightly displaced from the diagonal. This could be due to the presence of a small additional exon.

Figure 1. NORTHERN ANALYSIS

RNA was extracted from uninfected (control) or B19 infected total bone marrow cells and 3 ug of total RNA applied to each lane of a 1.5% formaldehyde gel. Samples were hybridized with ^{32}P-labeled pYT103 after transfer to nylon paper.

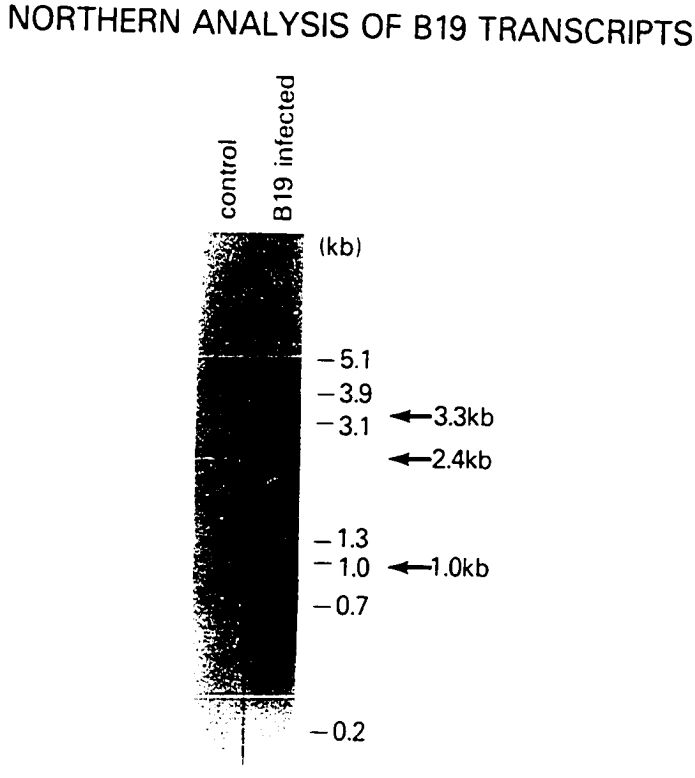

Figure 2. S1 Analysis

This figure illustrates the S1 analysis of B19 transcripts using a full length B19 DNA probe (pYT103 insert). 5 ug of total RNA from uninfected bone marrow (control) or 0.5 ug (left lane) and 2 ug (right lane) from the B19 infected samples were hybridized with 0.1 ug of pYT103 DNA. S1 protected fragments resolved in (A) neutral and (B) alkaline 1.5% agarose electrophoresis followed by Southern transfer and hybridization with ^{32}P-pYT103 probe. (C) Two dimensional S1 analysis of 3 ug of total RNA from infected bone marrow cultures. The lower panel shows a longer exposure of a portion of the upper panel. The diagram indicates the location of transcripts and exons.

Figure 2A,B.

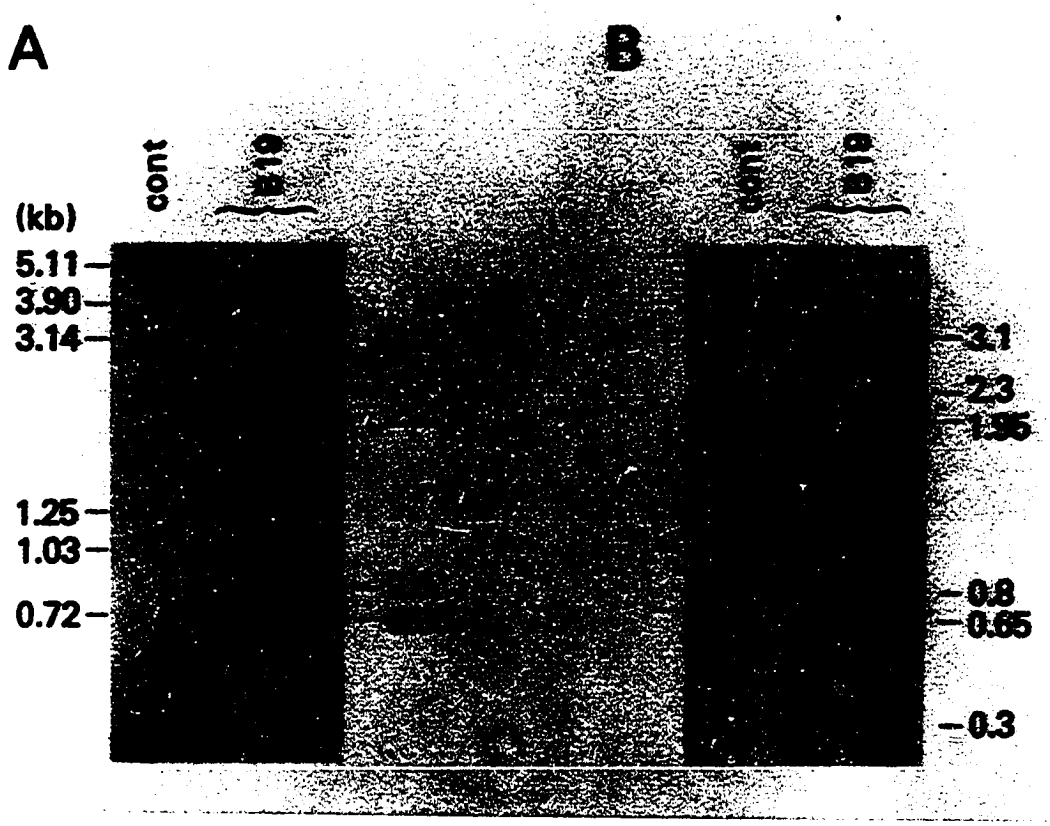

Figure 2C.

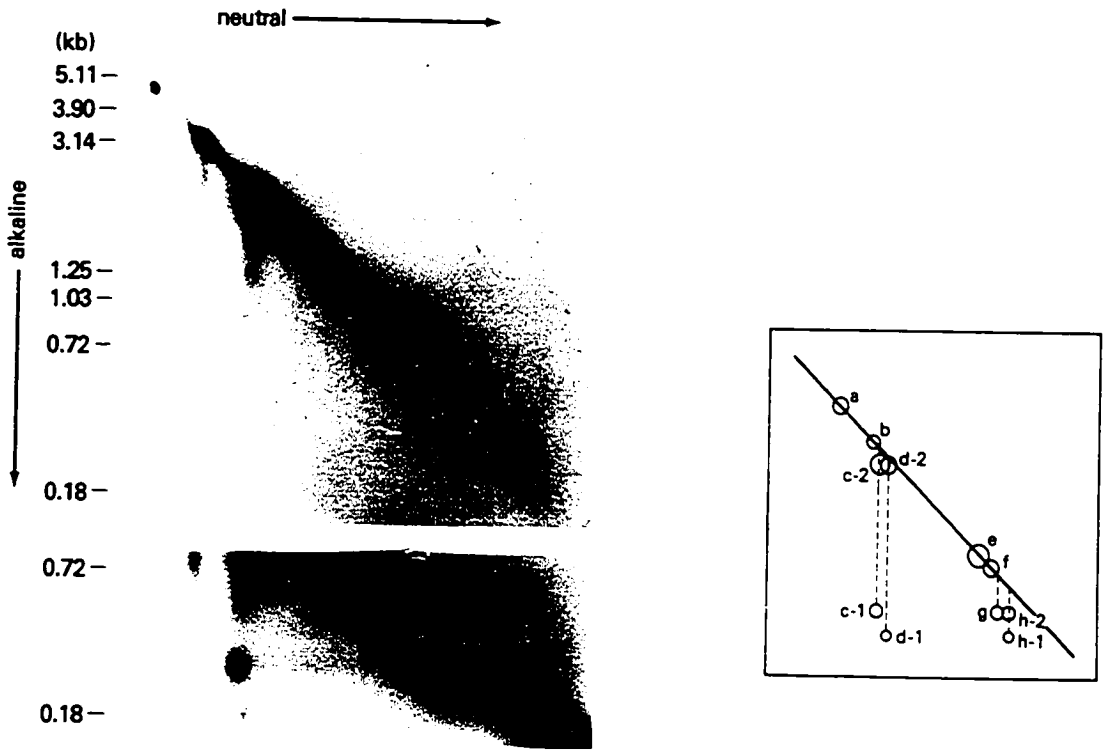

Crude Mapping of B19:

A crude map of B19 (human) pathogenic parvovirus was constructed from rehybridization studies. Cloned B19 DNA (pYT101 and pYT103) was subjected to restriction enzyme digestion. This digestion yielded five DNA probes which represented different regions of the genome from map units 10 to 100 (Fig. 3). The probes were used to analyze two dimensional S1 gels by successive rehybridization of the same filter. Fig. 3A and 3B reveal representative results for two of the probes. The far left hand probe (I) detected only the single RNA species, b, of 2.3 kb (Fig. 3A). The far right hand probe (V) detected five transcripts as shown in Fig. 3B. These were 3.1 or a, the 1.95 exons of c2 and d2, and two different 0.3 exons from g and h2. The summary of all hybridizations is shown in Fig. 3C. These results suggested that three B19 RNA species (b,e,f) terminated in the middle of the genome. This contradicts the pattern of cotermination near the right hand terminus of all RNA species observed with other Parvoviridae such as AAV2 and MVM. All the RNA transcripts from AAV2 (36) and MVM (34) terminate near the right hand of the genome.

From the crude map of the right side of the genome, species a, c, d, g, and h were expected to have similiar initiation and termination sites, but introns of at least two different sizes (small for c and d, large for g and h) and the absence of an intron for transcript a were predicted (Fig. 3C). A probe that extends from m.u. 9 to 95 was used. On alkaline gels, this probe gave the 3.1 kb band of much higher intensity after exonuclease

Figure 3. REHYBRIDIZATION

The filter shown in Figure 2 was repeatedly rehybridized with shorter than full length probes, shown in panel C. Two examples of the results are shown: (A) probe I; (B) probe V. All results are summarized in (C). The boxes represent predicted RNA structure and the +, +/-, and - signs represent the strength of hybridization with different probes. Map units are calculated based on the assumption that the genomic length of B19 is 5.4 kb, such that 1 map unit = 0.054 kb or 54 bases. pYT103 corresponds to m.u. 0-95 while pYT101 to map units 72-100.

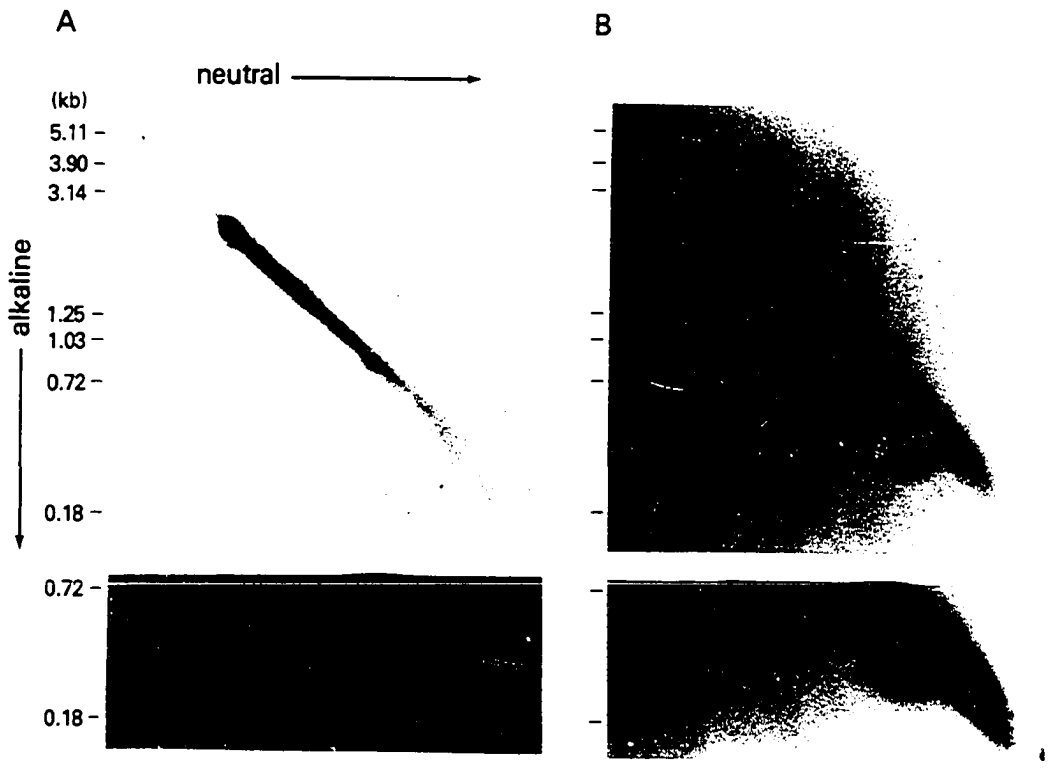

Figure 3C.

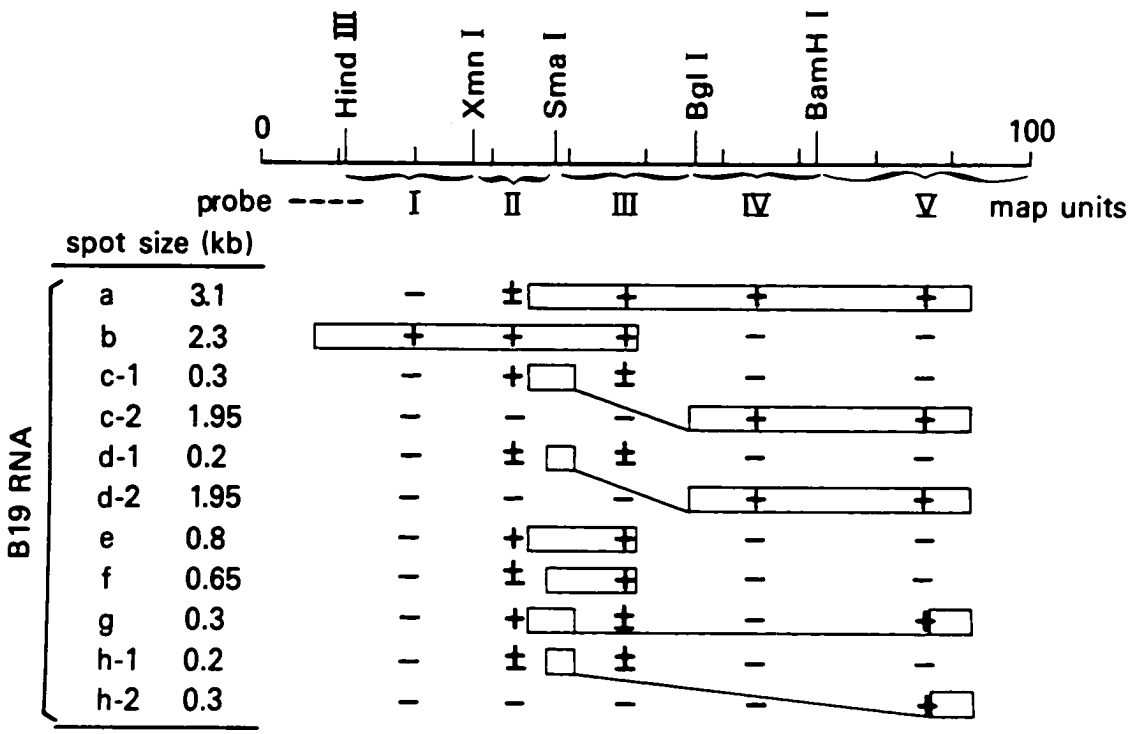

Figure 4. EXONUCLEASE VII ANALYSIS

RNA-probe DNA hybrids were digested with exonuclease VII, which in contrast to S1 nuclease does not cleave within introns.

(A) Alkaline gel electrophoresis of protected fragments of two probes, a and b, are shown.

(B) Two dimensional exonuclease VII analysis showing separation of the components of the dense 3.1 and 2.3 kb bands seen on the one dimensional gel, as well as discrimination of hybrids of probe length.

Figure 4A.

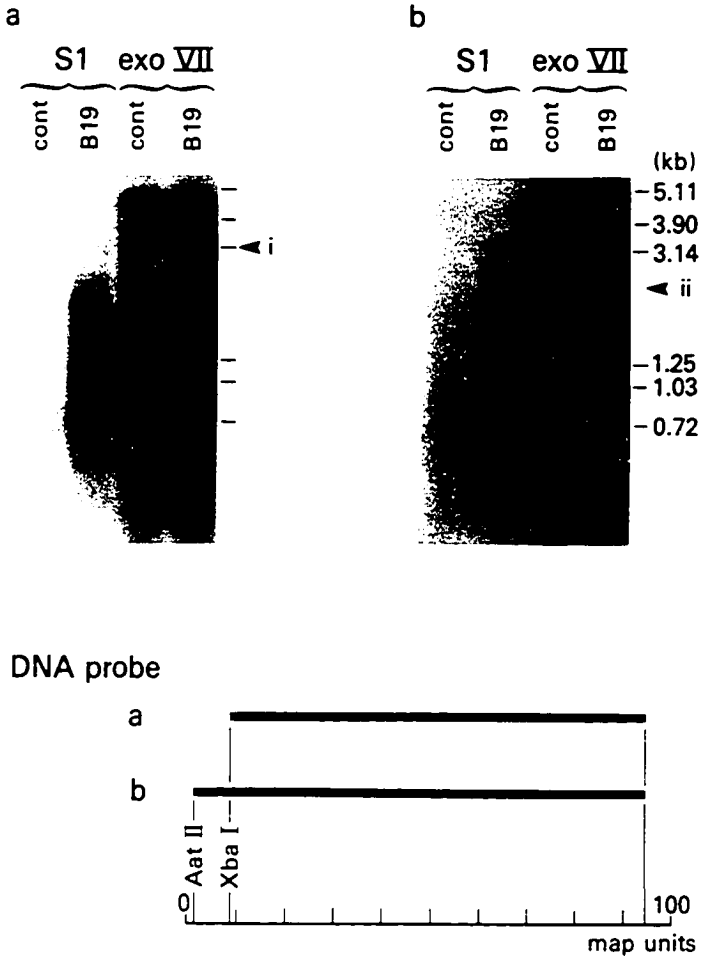

Figure 4B.

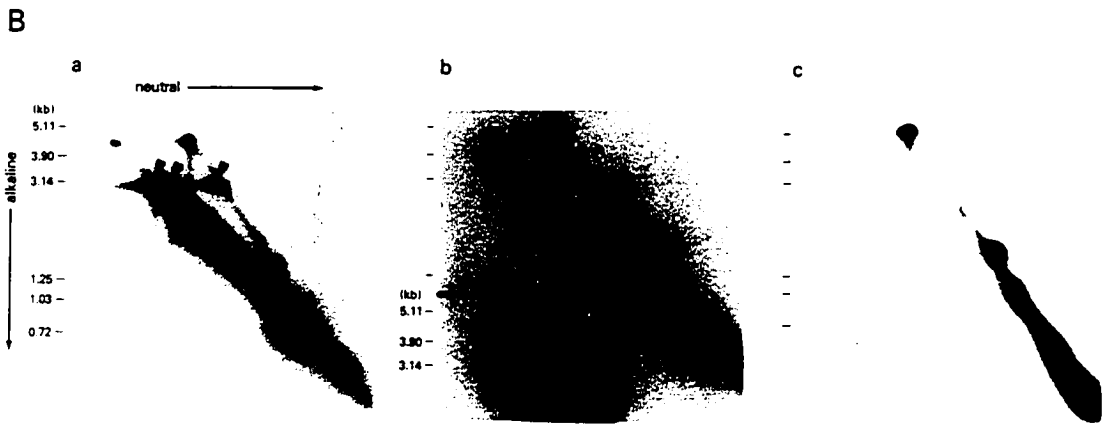

VII digestion than after S1 nuclease digestion, suggesting overlap of these five species (Fig. 4A-a). Overlapping was demonstrated by the separation of the 3.1 kb species into three groups on two dimensional gels; the three discrete spots probably correspond to species a, c+d, g+h (Fig. 4B-a).

Precise Mapping of B19:

Based on the results of crude mapping, several small restriction enzyme fragments were prepared to precisely determine the location of the borders of the various exons. These fragments were used as probes after radioactive labeling at the 5′ or 3′ ends in S1 protection analysis (Fig. 5). Map units 6, 35, 37.5, 56, and 87 were analyzed as 5′ borders of exons and map units 40.5, 49, and 92.5 for the 3′ borders (Fig. 5A). Representative autoradiographs are shown in Fig. 5B and 5C for 5′ and 3′ probes respectively. All transcripts were detected with strand specific probes. This confirmed that only the minus strand of the virion served as a template for RNA transcription, as predicted from the open reading frames based on the nucleotide sequence (21).

A polyadenylation signal at nucleotide 4990 has been shown in the sequence of B19 (21). The 3′ border of exons at map unit 92.5 were located just downstream of this signal. The 3′ border of exons at map unit 49 coincided with unusual polyadenylation signal at nucleotide 2639 (ATTAAA) and at nucleotide 2645 (AATAAC). The unchanged size of 0.8 kb fragment protected by probe a, following exonuclease VII analysis, supported termination at this point rather than the presence of a large right side intron. The termination of transcript b, e, and f are

Figure 5. PRECISE S1 MAPPING OF EXON BOUNDARIES

(A) Probes employed for precise mapping of the 5′ and 3′ exon boundaries and their protected fragment sizes are shown below the B19 transcription map.

(B) Representative data from S1 analysis using 5′ end labeled probes. Probes XmnI-SmaI was used to determine the 5′ boundaries of transcripts a, a′, c, d, e, f, g, and h. Similarly probe HindIII - TthIII were used for a, a′, e, and f; probe RsaI - RsaI for c and d; and probe BamHI-ScaI for g and h. Also, probe AccI-HincII were used for a and a′.

(C) Autoradiographs from S1 analysis using 3′ end labeled probes. Probe AvaI-Tth111I was used for transcripts c, d, g, and h; probe AvaI-BglI for b, e, and f; probe ApaI-right end for a, a′, c and d; and probe BstXI-right end for g and h.

(D) Berk and Sharp S1 analysis for transcript b. Fragment Aat II-Nhe I was hybridized with RNA samples and S1 protected fragments resolved by Southern transfer and hybridization with ^{32}P-pYT103.

Figure 5A.

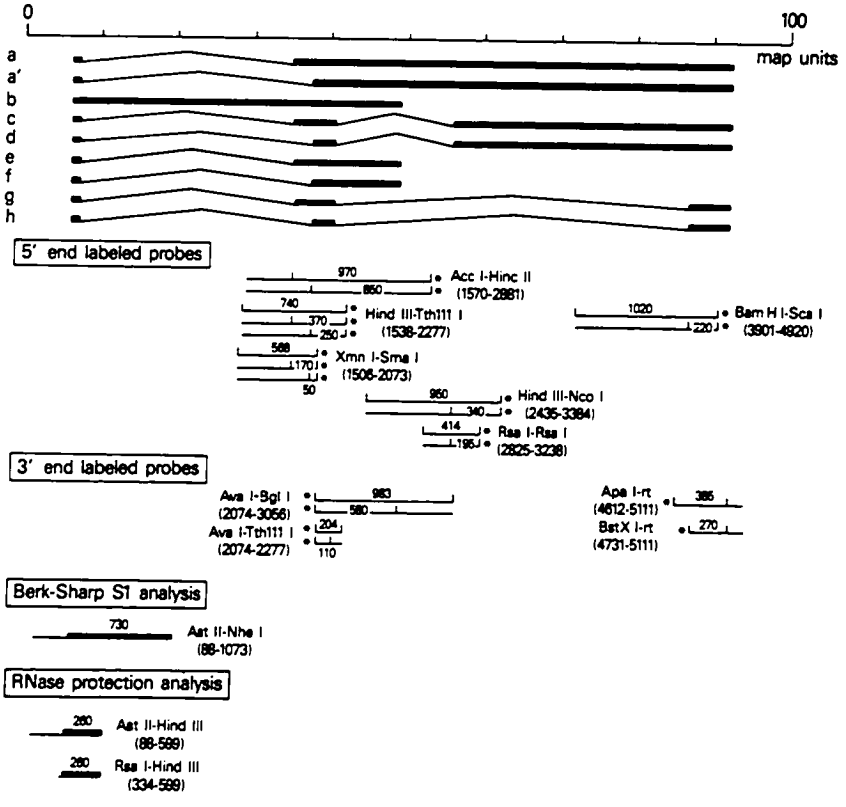

Figure 5B.

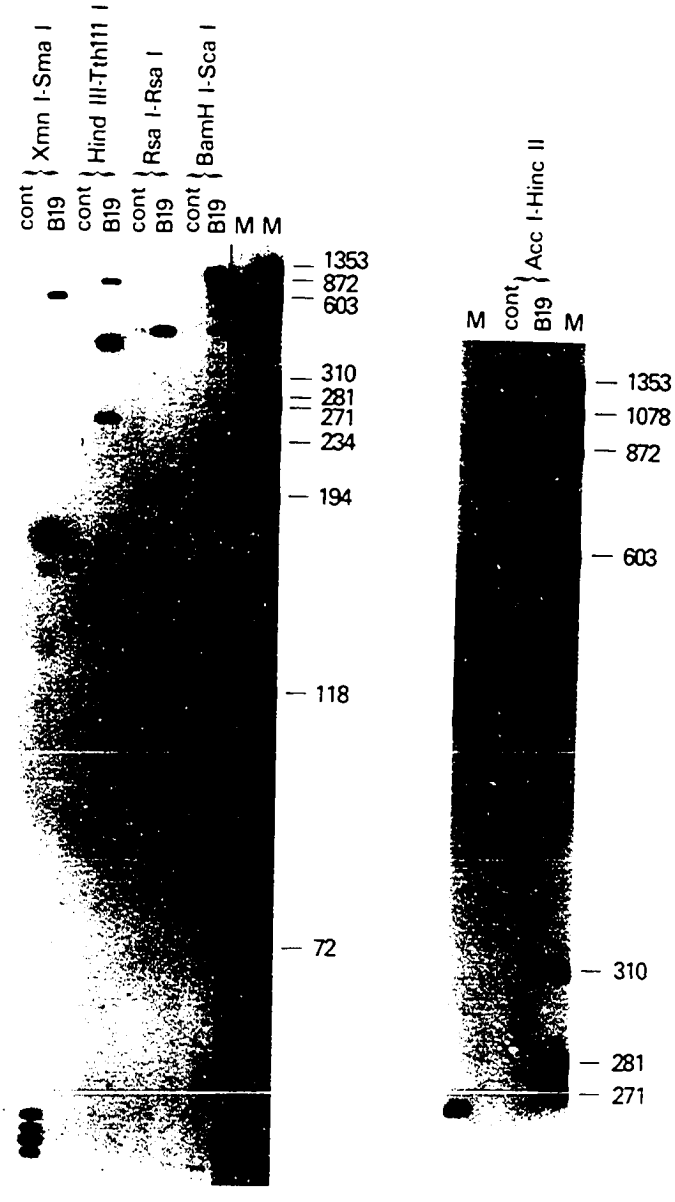

Figure 5C.

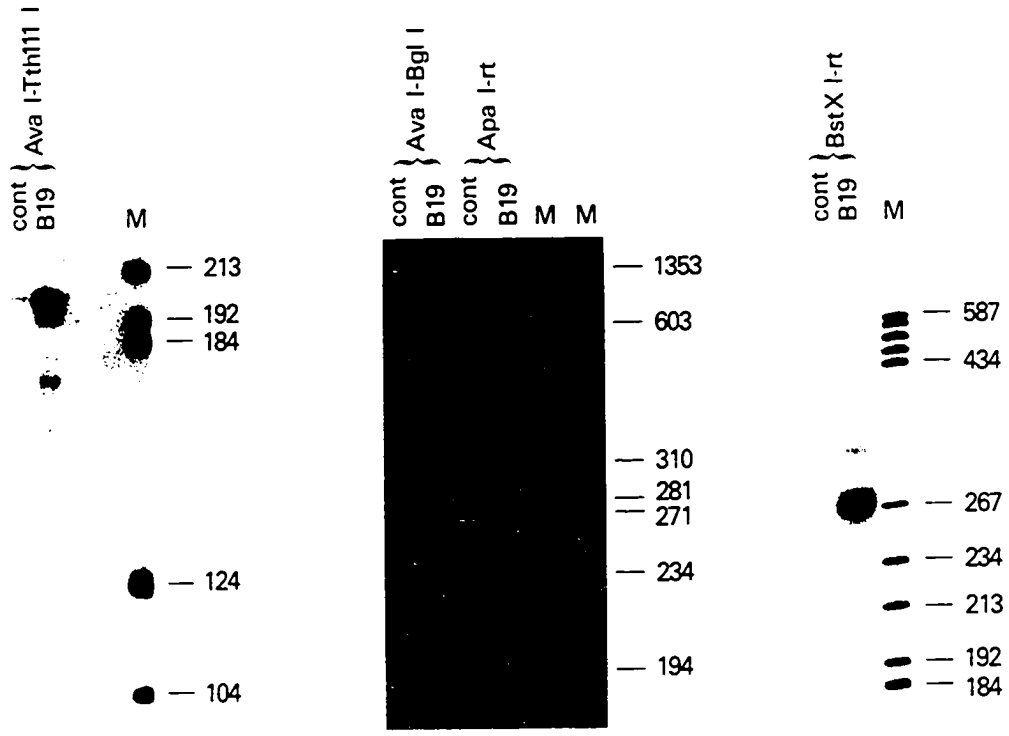

Figure 5D.

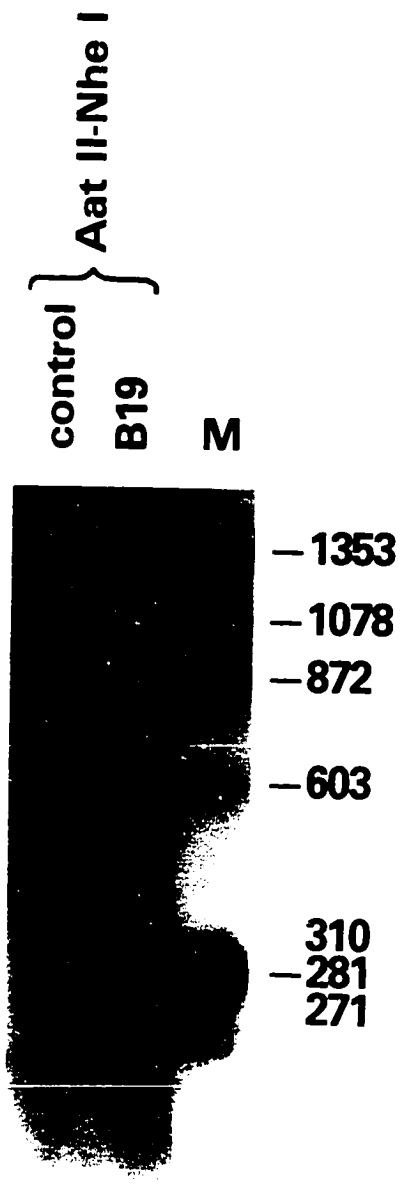

at the conventional map unit 92.5 polyadenylation site (Fig. 4A-a). The nucleotide sequence of B19 (21) shows several TATA-like sequences but only the far left side promoter was compatible with the 5′ border of RNA transcript b. This was around map unit 6. However, there is no suitable promoter like sequences located proximal to the 5′ borders of transcripts at map units 35 and 37.5. The nearest upstream TATA sequence was almost 700 nucleotide distant; other nearby promoter like sequences were located within the transcription unit.

Short Leader Sequences:

Most of the B19 transcripts have short leader sequences. The presence of short leader sequences was shown by primer extension experiments. Results showing comparison of primer extension and S1 nuclease analysis are shown in Fig. 6. One example of the interpretation of these experiments is given for the a, a′, e, and f transcripts. In S1 nuclease analysis using the 5′ end labeled HindIII-Tth111 I probe (nucleotides 1538-2277) resulted in two different sizes of the reverse transcripts of 430 and 305 nucleotides, both about 50-60 nucleotides longer than the S1 protected fragments. Similiar differences of about 50 bases were found for all the RNA species examined which included a, a′, c, d, e, f, g, and h. Exonuclease VII analysis helped determine the location of these 50-60 nucleotide exons.

After hybridization and enzymatic digestion, conflicting results were obtained with the XbaI right hand end (map units 8.9-94.6) probe and a slightly longer AatII right hand end (map units 1.7-94.6) (Fig. 4A,B). On alkaline gels, experiments with

Figure 6. PRIMER EXTENSION ANALYSIS

This analysis was used to demonstrate short leader sequences or exons by comparison with S1 protected fragments.

(A) For transcripts a, a', e, and f, a fragment from nucleotides 1538-2277 was used for S1 protection experiments and a much shorter fragment, nucleotides 2076-2277, was used as a primer to generate reverse transcripts. Although transcripts a and a' are much less abundant than transcripts e and f, the same size bands observed with S1 protected fragmentswere not seen even with much longer exposures.

(B) For transcripts c and d, S1 analysis was done with fragment 2435-3384, primer extension with 3110-3384. S1 analysis showed a single fragment 340 nucleotides from the far right side main exon. Primer extension showed two larger fragments, 670 and 550 nucleotides.

(C) For transcripts g and h, S1 analysis was done with fragment 4608-4920, primer extension with 4727-4920. Results are comparable to those obtained in (B).

Bands which appeared in both control and infected lanes were considered artifacts of the primer extension reactions, as they appeared also on addition of tRNA alone.

Figure 6.

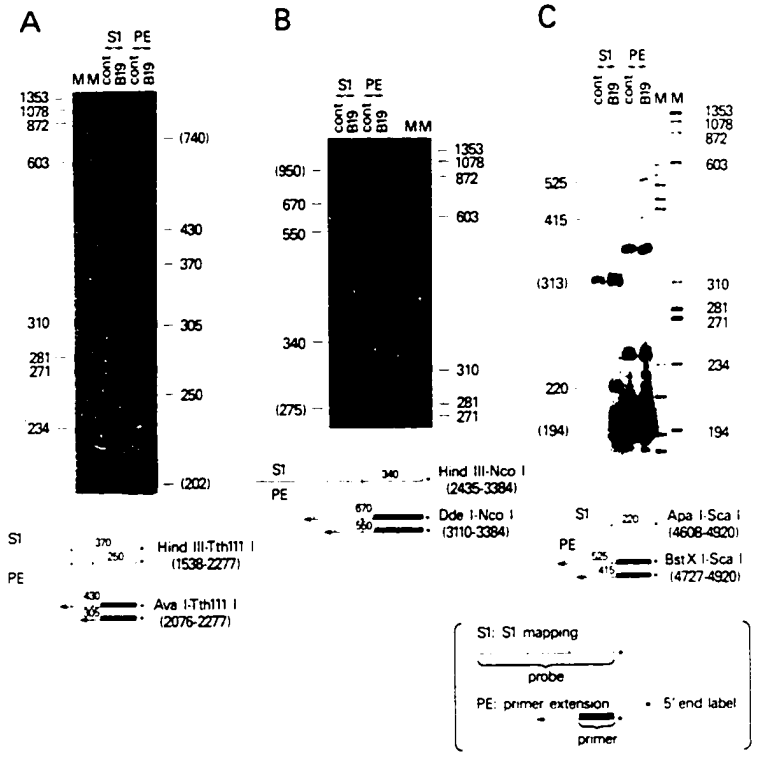

the longer probe (Fig. 4A-b) resulted in the appearance of a heavy band at 2.3 kb. This band was separated into two spots on two dimensional gels (Fig. 4B-b). The denser spot probably represented the major transcripts e and f, the lighter spot the most minor transcript b. Similarly, the presence of short 5' exons for transcripts which terminated at the right end (a, c, d, g, h) were predicted to result in exonuclease VII protected fragments of approximately probe size (AatII-right hand end) or full genomic length. On one dimensional gel these could not be discriminated from reannealing of the probe (Fig. 4A-b). However, in two dimensional analysis, with the longer probe, three spots at 4.7 kb were apparant. These were slightly shorter than the probe length of 5 kb and probably corresponded to transcripts a, c+d, and g+h (Fig. 4B-b). The 4.7 kb or 2.3 kb multiple spots were not observed with hybridization using the slightly shorter XbaI probe (Fig. 4A-a, 4B-a). The short exons for all transcripts were therefore localized to the region between map units 1.7 and 8.9.

RNase protection analysis provided additional proof of the short 5' exon in this region. This RNase analysis was carried out with a uniformly labeled RNA probe corresponding to the restriction fragment AatII-HindIII (nucleotides 88-599) (Fig. 7). Two protective fragments were found to be present - one was about 60 nucleotides and the other was about 260 nucleotides and derived from minor transcript b. Using several different restriction fragments from this region, leader sequences were localized to lie between nucleotides 340 and 410. This result

Figure 7. RNase PROTECTION ANALYSIS

The figure shows RNase protection analysis of the left side leader sequences. Uniformly labeled RNA probes extending from or within the region from nucleotide 88 to 599 (shown below) were hybridized with RNA from infected marrow cells or control RNA (tRNA alone or uninfected HeLa cell RNA). RNase protected fragments were resolved in polyacrylamide-urea gels. For the leader sequences, two probes detected fragments of the same size of about 60 bases (AatII-HindIII and RsaI-HindIII); the BstNI-HindIII probe detected a fragment of about 35 bases; there was no apparant band with hybridization to the HincII-HindIII probe. For transcript b, the 260 bases protected fragment also was approximately shortened with the same probes. Open arrows and boxes indicate protected fragments of transcript b, solid arrows and boxes protected fragments for the short leader sequences.

Figure 7.

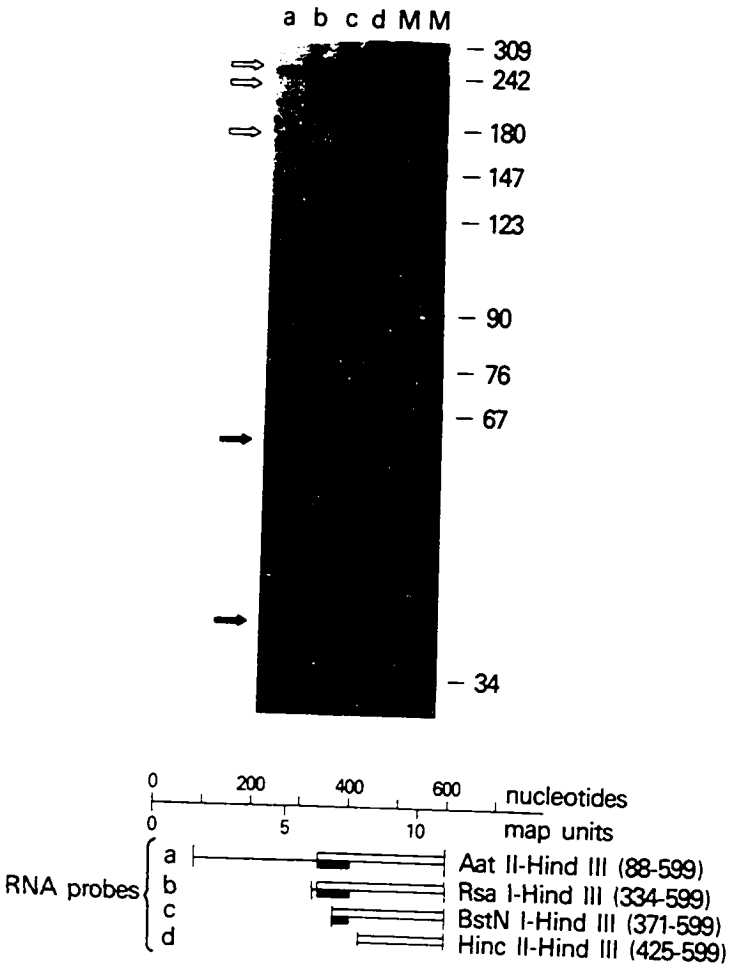

Figure 8. PROMOTER FUNCTION

This figure illustrates promoter function in transient CAT expression assay. Vectors were constructed, linked to the CAT gene, and transfected by calcium phosphate mediated transfer into HeLa cells (A) or by electroporation into human erythroid bone marrow cells (B).

(A) (a) pUC-9 control;

(b) LB-cat, which included a left-side promoter;

(c) XA-cat, including upstream sequence of the middle exons, excluding the far left side promoter;

(d) Co-transfection of XA-cat with a vector that expressed the major non-capsid protein of 77 kd (map units 0-58);

(e) LA-cat, which comprises map units 0-38, contained the left promoter, and a frame shift mutant at map unit 29;

(f) pRSV-cat, positive control CAT vector; and

(g) enzyme control.

(B) (a) LB-cat, co-infected with B19;

(b) XA-cat, co-infected with B19;

(c) pRSV-cat, co-infected with B19; and

(d) enzyme control.

Figure 8.

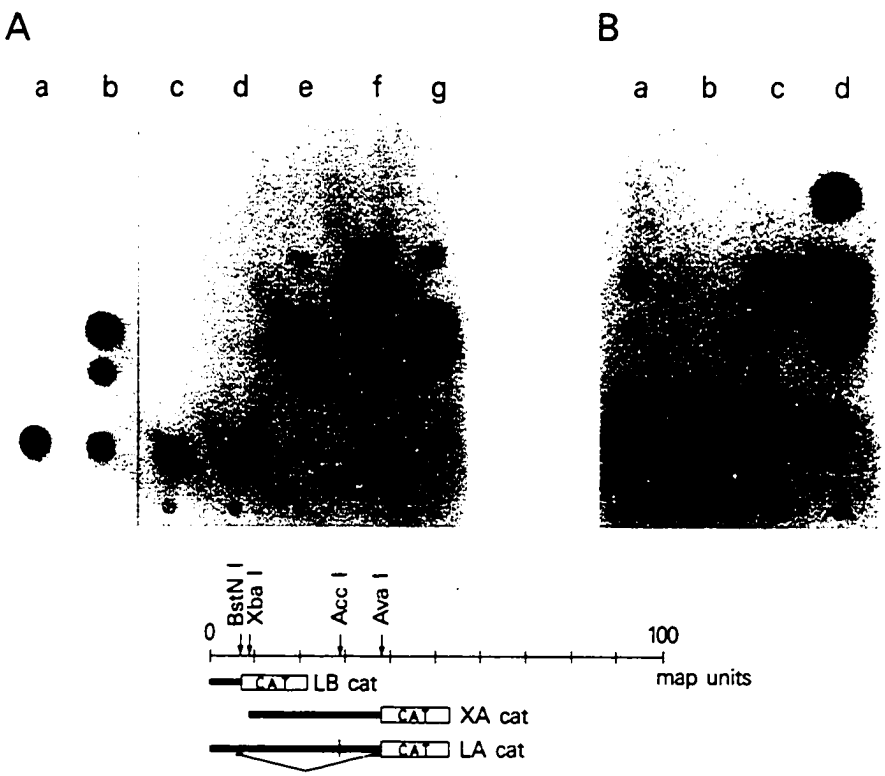

indicated as a functional promoter the TATA sequence at nucleotide 319. In addition, this site corresponded to the 5' exon border of the single unspliced transcript b, suggesting common origination of all B19 transcripts at map unit 6.

Left Side Promoter for B19 Transcription:

The transcription map suggests that all B19 transcription is driven from a left side promoter at about map unit 6. In addition there is little evidence of initiation of transcription in the middle of the genome from an internal promoter, which is characteristic of other animal parvoviruses. Functional promoter assays were performed using vectors constructed from various putative B19 promoter sequences linked to the chloramphenicol acetyltransferase gene (CAT) (Fig. 8). A construct including the far left side of the genome (map units 0-7; LB-cat) expressed CAT efficiently in HeLa cells and CAT activity was detectable in fresh erythroid bone marrow. A construct that included map units 9-38 (XA-cat), but lacked the left side promoter, was not active in either cell type. Generally, the middle promoter appears stronger than the left side promoter in animal parvoviruses. While the signal from the B19 P6 promoter in bone marrow cells was faint, failure to detect a concomitant signal from the middle promoter in bone marrow cells suggested the absence of a functional promoter in this region.

Another construct of map units 0-38 and containing the left side promoter was made (LA-cat). A frame shift mutation was made in it at the AccI site to block translation initiated from the ATG at nucleotide 436 (map unit 8). However, very efficient CAT

expression by LA-cat vector was observed in HeLa cells. Expression under these conditions was possible only with splicing of an intervening sequence between the left side promoter and the CAT gene. This shows that the left side promoter could be used for transcription for transcript b and transcripts with major exons starting at map units 35-37.5.

Coding of B19 Proteins:

The B19 capsid proteins are encoded by the right side of the genome (38). Transcripts a and a' (Fig. 9) are probably responsible for encoding the 84 kd capsid protein. As the first five ATGs are followed shortly by in frame termination, the sixth ATG in a Kozak sequence (37) is probably used. This sixth ATG is located at nucleotide 2444. The transcripts c and d may encode for the 58 kd major capsid protein. The sixth ATG codon is spliced out and the first appropriate ATG codon at 3125 in reading frame is probably used. The first ATG occurs at nucleotide 436 for transcript b (37)(purine-NNATG). From construction of vectors containing B19 sequences and their mutants and analysis by immunoprecipitation of B19 specific proteins after transfection into HeLa cells, the 77 kd major non-capsid protein could be assigned to transcript b (Shimada et al, Manuscript in preparation). The ATG at nucleotide 436 in reading frame 3 represented the translation starting codon for this protein. This was determined by promoter deletion and frame-shift mutation experiments (Shimada et al., manuscript in preparation).

Figure 9. TRANSCRIPTION MAP OF B19 PARVOVIRUS

Transcripts are ordered by length. Shown is the location of the P6 promoter, functional polyadenylation signals, splice donor and acceptor sites, open reading frames (boxes), ATG sequences (vertical lines), PuNNATG (Kozak consensus sequence [37], open triangles), and translation initiation and termination sites, which are defined by the limits of the shaded areas of boxes showing open reading frames. Frame numbers are indicated within the boxes. For the TATA sequences, the bold line indicates the functional promoter while the thin lines show other non-functional TATA regions. Similarly, for potential polyadenylation signals, the solid bold line indicates the functional conventional site, the open line the variant and functional polyadenylation site, and the thin lines non-funtional AATAAA sequences.

Figure 9.

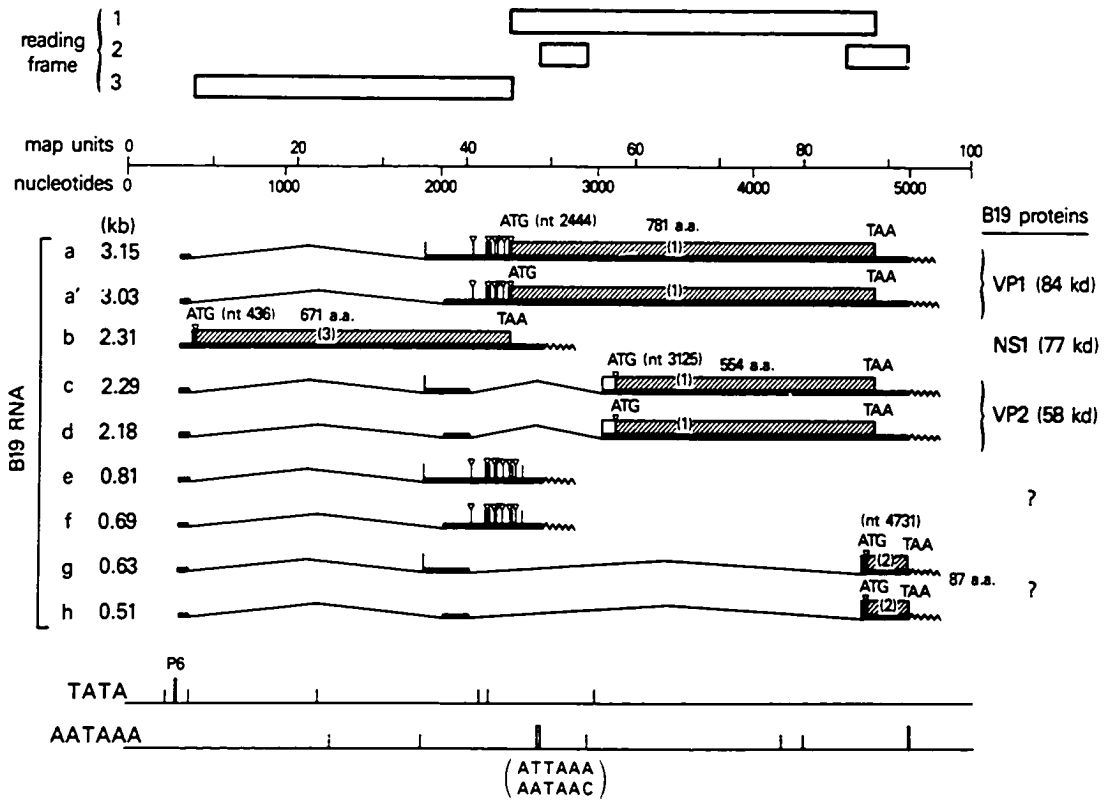

The transcription map of B19, including functional promoter site, polyadenylation signals, splice sites, and open reading frames is shown in Fig. 9.

OVERLAPPING TRANSCRIPTS

Two dimensional gel exonuclease VII analysis was performed for mapping of overlapping transcripts with the same initiation and termination sites and with or without introns of differing size. Plasmid pTZ.BS and two deletion mutants, pTZ.NBdel and pTZ.NAdel, were constructed (Fig. 10) as shown in methods. BS, NBdel and NAdel represent three in vitro transcripts obtained from pYT103. To use a model system, BS represented unspliced RNA, while NBdel and NAdel represented spliced RNAs. NBdel was missing the nucleotide sequence between the NcoI and BglII sites while NAdel had the nucleotides between NcoI and ApaI sites deleted from its sequence. The three RNA species had the same transcription initiation and termination sites, but NBdel contained a small intron while NAdel contained a large intron.

Formaldehyde gel electrophoresis (Fig. 11) was performed to determine the size of the RNAs which showed that BS was 1.9kb, NBdel was 1.3 kb, and NAdel was 0.6 kb. These values are in agreement with expected values from plasmid DNA sequences. Exon size was determined by S1 alkaline gel analysis (Fig. 12). As expected, BS had an exon of 1.9 kb; NBdel had two exons, 0.3 and 1.0 kb; and NAdel had two exons of 0.3 kb each. Exonuclease VII analysis of these RNAs produced a 1.9 kb band for all species.

Figure 10. PLASMID CONSTRUCTIONS & IN VITRO TRANSCRIPTS

Plasmid constructions are shown along with their corresponding in vitro transcripts. The insert portions of each of the three constructs are shown above the diagram of the pTZ19R multifunctional vector. Synthetic transcripts were obtained by T7 RNA polymerase treatment. The in vitro transcripts (unspliced) correspond to in vivo transcripts with no intron (BS), a small intron (NBdel), and a large intron (NAdel). The size of the transcripts and exons are shown.

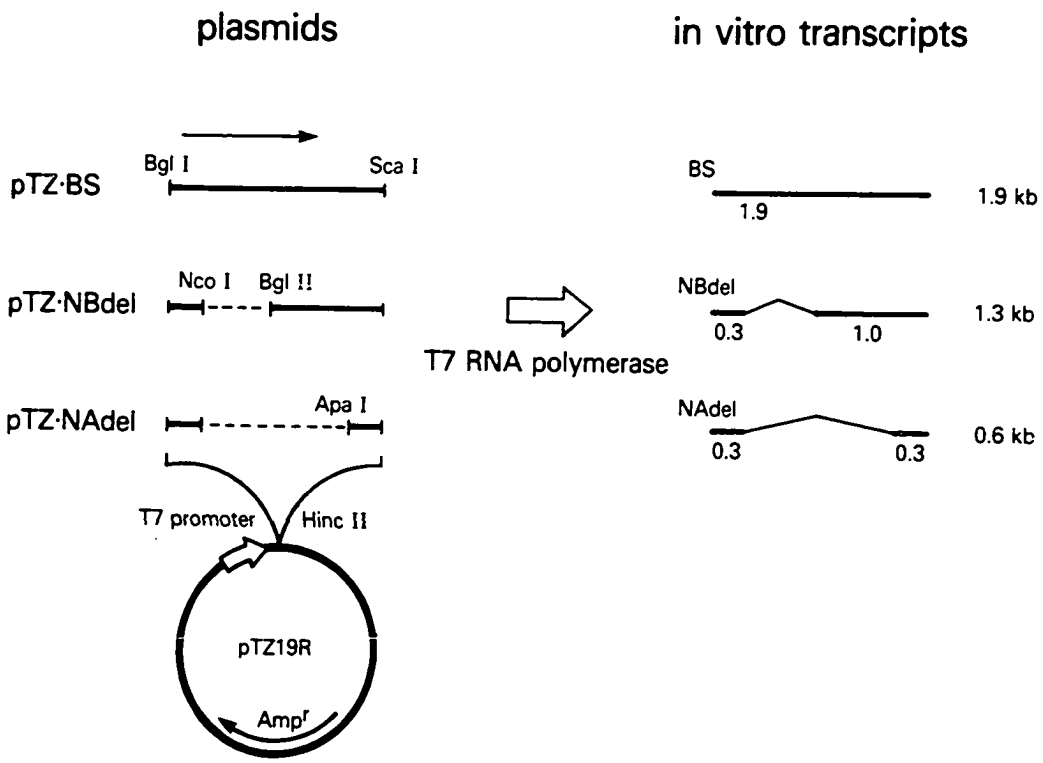

Figure 11. DETERMINATION OF RNA LENGTH

This figure shows the determination of RNA length by 1.5% formaldehyde-agarose gel electrophoresis. An RNA ladder was used for molecular weight standards.

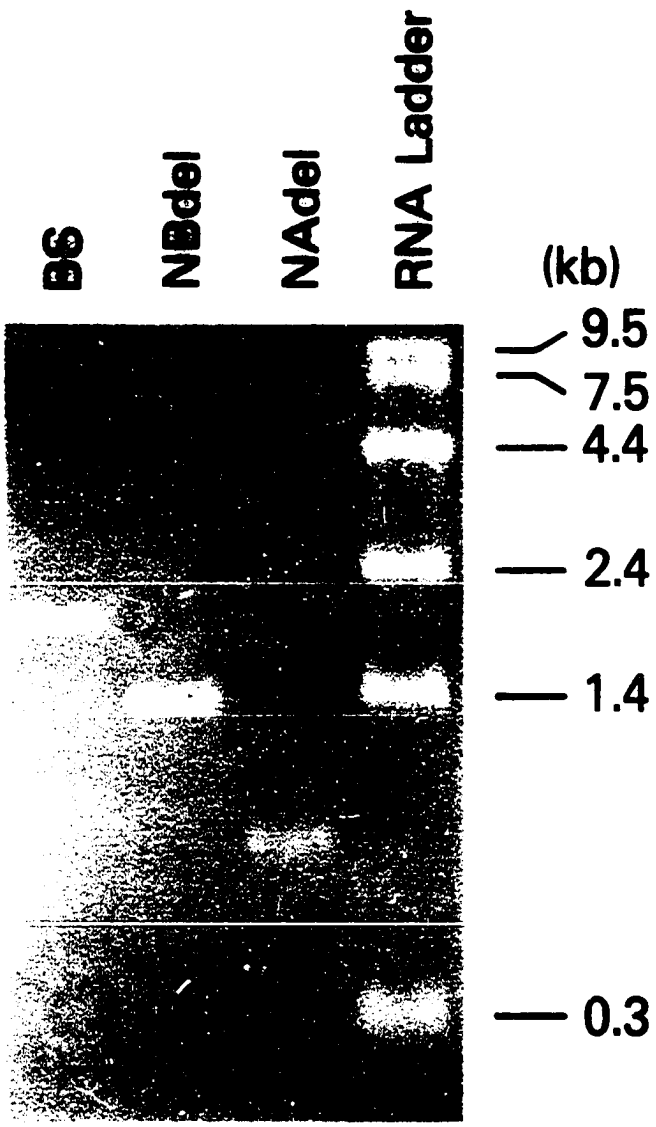

Figure 12. DETERMINATION OF EXON SIZE

S1 alkaline gel analysis is used in this figure to determine the exon size.

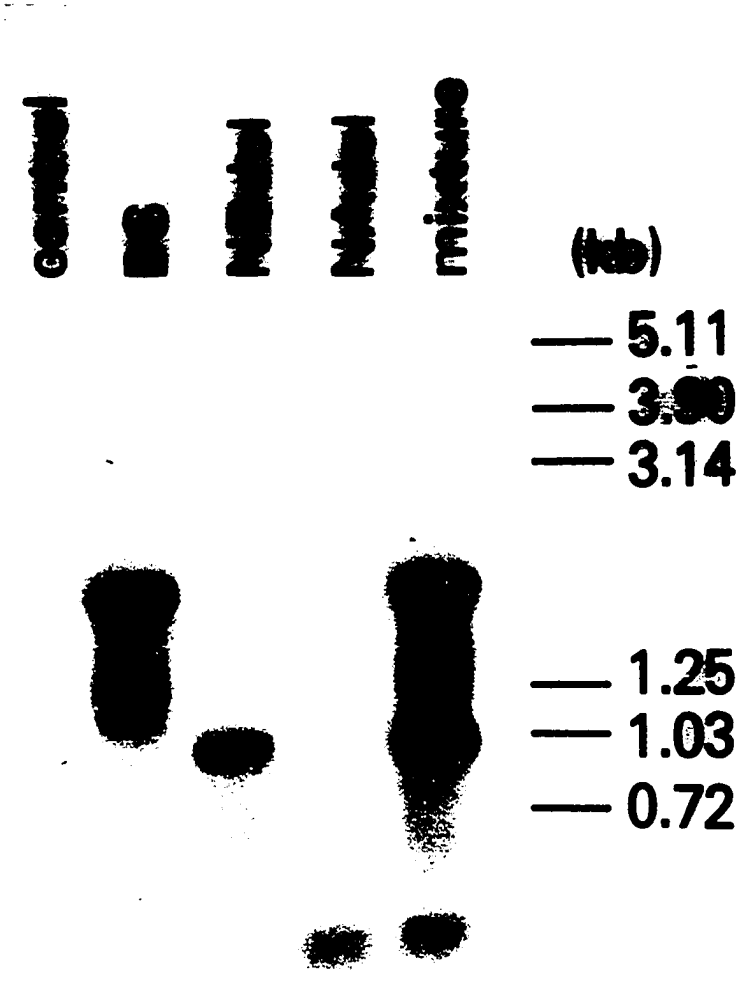

Figure 13. TWO-DIMENSIONAL EXONUCLEASE VII ANALYSIS

This figure illustrates the two-dimensional analysis of RNA transcripts with and without introns.

(A) BS RNA.

(B) mixture of BS, NBdel, and NAdel.

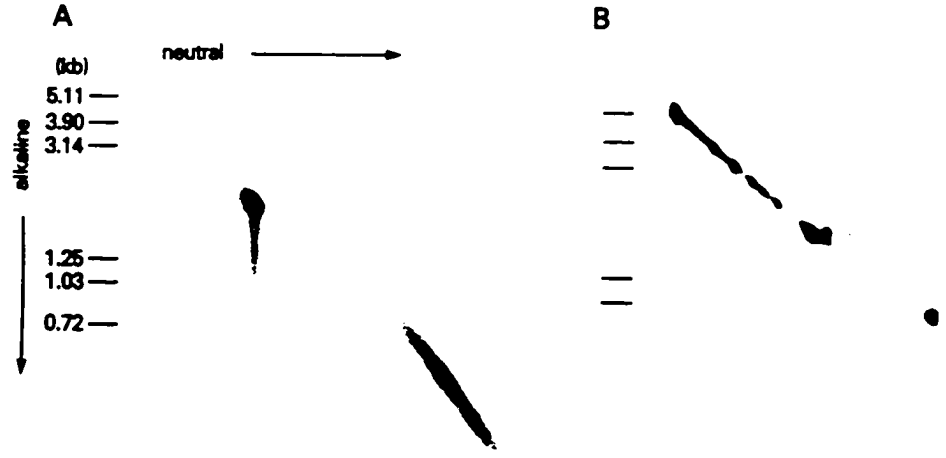

Two-dimensional analysis was performed after exonuclease VII digestion (Fig. 13). When the BS RNA was tested (Fig. 13) a single spot appeared on the diagonal axis. On analysis of the mixture of the three species (Fig. 13) the single spot seen on one-dimensional alkaline gel was now resolved into three distinct spots.

TRANSLATIONAL REGULATION

The genomic organization of B19 parvovirus has been established above. It has been shown that all transcription is driven from a single promoter at the far left side (P6) of the genome. The single unspliced transcript for the nonstructural protein is least abundant. VP2 transcripts are about five times more abundant than VP1 transcripts by densitometric determination in S1 alkaline gels. The nonstructural protein(s) are encoded by the left side of the genome and the capsid proteins by the right side. The first AUG codons in appropriate contexts (Kozak consensus sequence, purine-NNAUGN) are probably used for initiation of non-structural protein and VP2 translation.The region about 250 bases upstream of the predicted initiation site of VP1 contains seven AUG codons, five of which are in appropriate consensus sequences. These seven AUG codons are followed by in-frame termination codons that create multiple minicistrons (Fig. 14A). This region is suspected of regulating

Figure 14(A). UPSTREAM NONCODING REGION OF VP1 RNA

The sequence surrounding the AUG codons are shown, and the minicistrons are indicated below. The insert portions of the pTZ plasmids have been aligned with the map. The dotted line indicates the region deleted in the construction of pTZSR(THdel) and mu shows the location of a frame shift mutation at nucleotide 2430 (m.u. 45) for pTZSR(Hmu) to alter the location of the termination codon of the last minicistron. Relative rates of translation in vitro are shown by the solid arrows.

Figure 14(B). UPSTREAM NONCODING REGION OF VP2 RNA

In the native B19 molecule the region containing spurious AUG codons is removed by splicing. For the plasmids pTZSHBR, the upstream spurious AUG region of VP1 has been linked to VP2. pTZSHBR(2) and pTZSHBR(3) differ in the reading frame of the last minicistron, which alters the degree of overlap of the minicistron with the coding region of VP2.

Figure 14A.

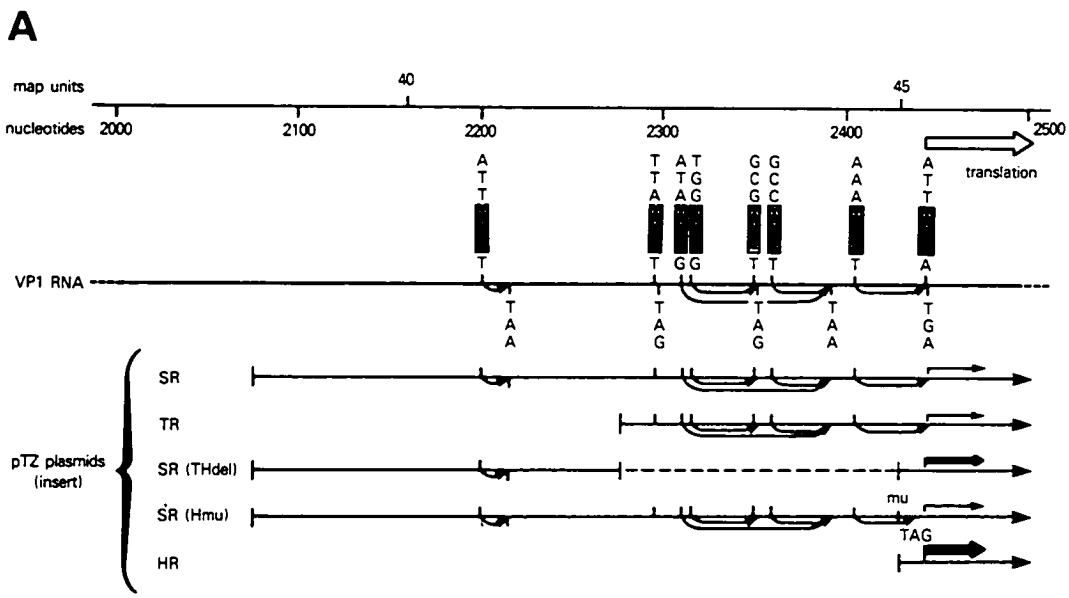

Figure 14B.

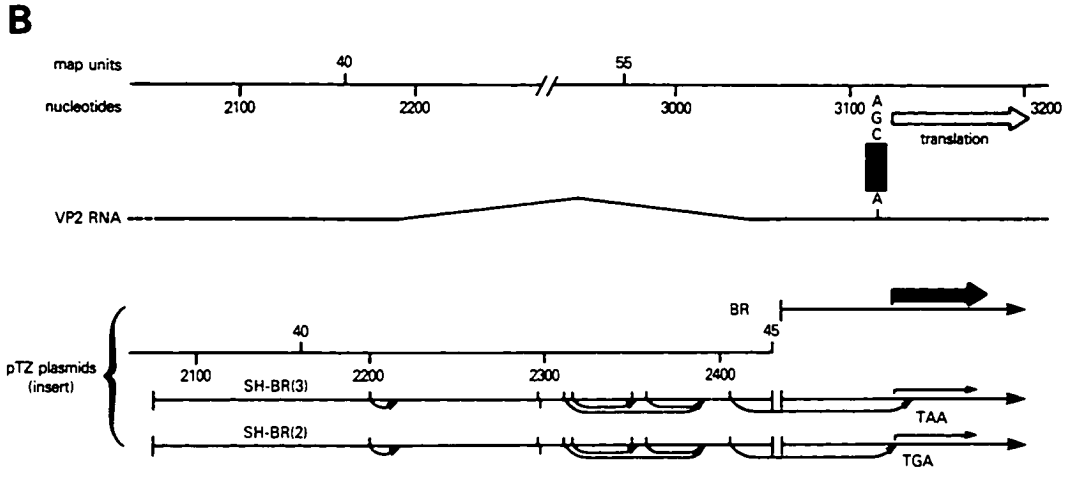

Figure 15. IN VITRO TRANSLATION OF SYNTHETIC RNAs

This figure shows the in vitro translation of VP1 (SR) and VP2 (BR) RNAs. The total and B19 specific protein products are shown in the autoradiograph of an 8% SDS-polyacrylamide gel. The same amounts of RNA templates were employed. Control lanes lacked RNA templates.

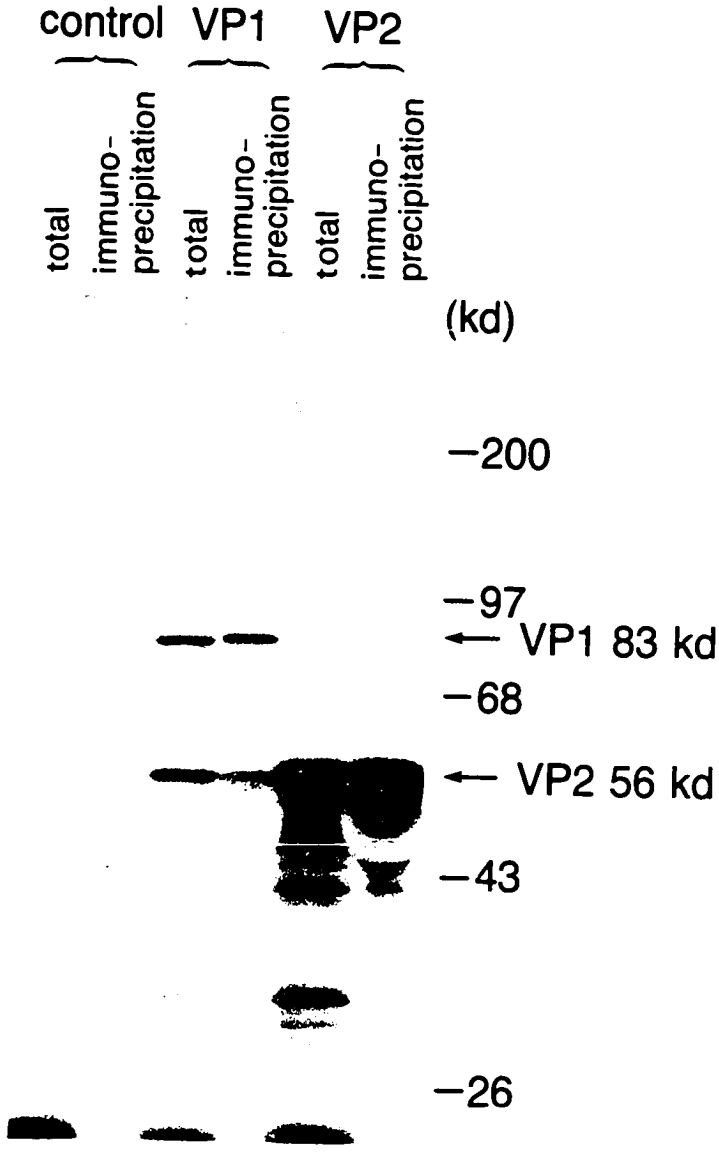

Figure 16. INCREASED TRANSLATIONAL EFFICIENCY

Increased translational efficiency of VP1 RNA after removal of upstream noncoding region. Reactions were terminated at 20 (a) or 60 (b) minutes. Two different experiments are shown which used different batches of reticulocyte lysate.

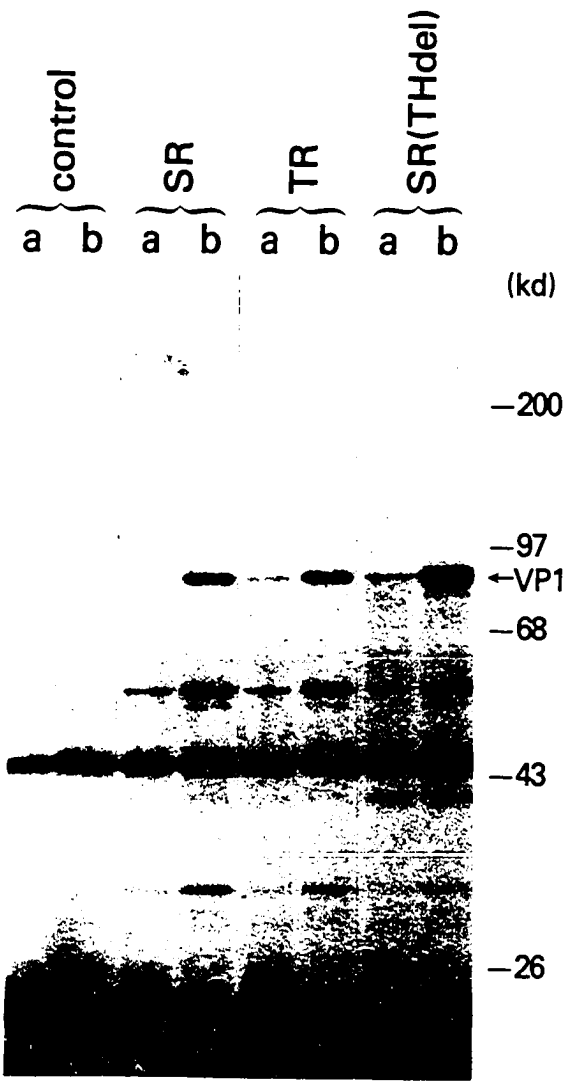

Figure 16B.

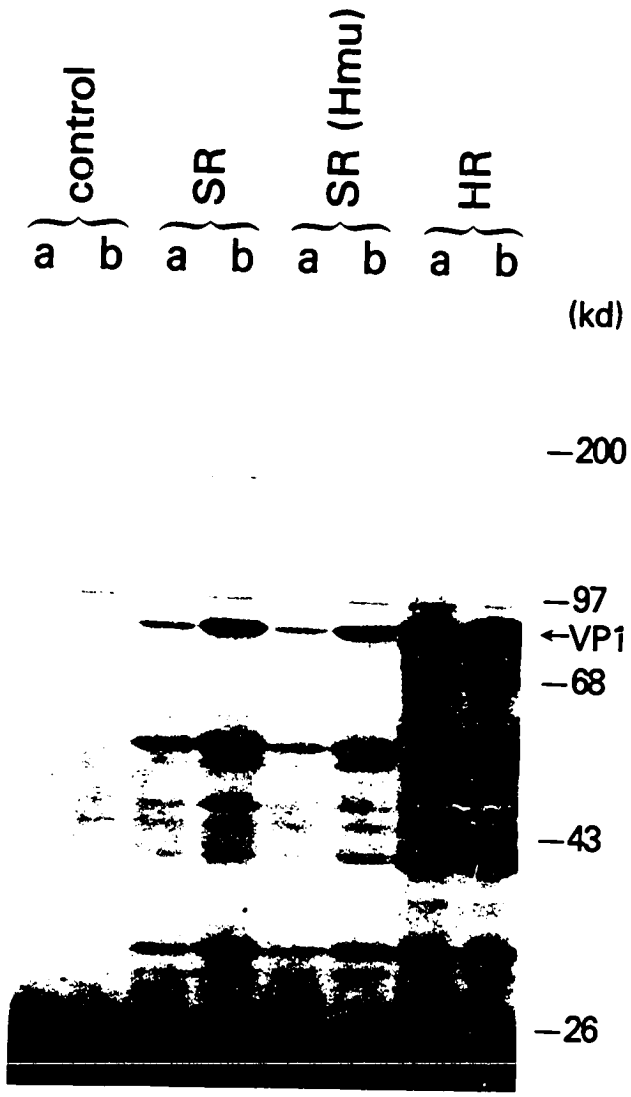

VP1 production. The position and context of authentic initiation codon influence translational efficiency. If the context is not favorable leaky scanning might occur and might regulate VP1 production. The seven AUG codon region is removed by splicing of the VP2 mRNA.

A fragment of pYT103c (map units 38-95) was subcloned into pTZ19R to produce VP1 synthetic RNA (SR), while VP2 synthetic RNA (BR) was produced from subcloning pYT103c fragment from map units 57-95 (Fig. 14A,B). Much more VP2 than VP1 was produced when equal amounts of pTZ.SR and pTZ.BR were translated in vitro (Fig. 15). These translated proteins were established as B19 products by immunoprecipitation with a specific human antisera. The approximate ratio of VP2 to VP1 protein translation was about 30:1. This shows that the amounts of capsid protein are regulated at the translational level.

The plasmid pTZ.SR contained the original upstream sequences containing the seven spurious AUG codons. Several deletion mutants were made from this plasmid. They contained different numbers of the spurious codons and are shown in Fig. 14A. The RNA transcribed from these plasmids were tested using in vitro translation for VP1 protein production (Fig. 16A). Removal of a single AUG codon from the upstream sequence (TR) had no effect on translational efficiency when compared to that of SR. Removal of six AUG sequences in SR(THdel) increased protein synthesis 3-fold while a 10-fold (as compared to SR) increase was seen with HR where all the spurious AUGs were removed (Fig. 16B). These results suggested that the spurious AUG sequences negatively

regulated VP1 synthesis. Even a single AUG upstream of the initiation site could down regulate translation.

Since the kinetics of VP1 protein synthesis in vitro were unknown, VP1 was measured at two different time points - 20 and 60 minutes. This was done to avoid measurement of protein after production had reached a plateau. The results were similiar at both 20 and 60 minutes. The level of VP1 production in the absence of inhibitory upstream sequences was still lower than that of VP2. This is probably due to the more favorable contextual sequence for the initiation site of VP2 (AGGAUGA) compared to that of VP1 (ATTAUGA) (51).

According to Kozak (52) reinitiation of translation is more efficient when the termination codon of an upstream minicistron precedes rather than overlaps the translation initiation site. VP1 RNA contains such an overlap. To test this hypothesis, an insertion mutation was introduced at map unit 44 to alter the termination site of the last minicistron preceding the initiation site of VP1 and eliminate overlap. However, protein synthesis from this RNA, SR(Hmu), remained unaltered (Fig. 16B). This shows that the termination codon overlap does not reduce the efficiency of reinitiation of translation.

The upstream region containing the seven spurious AUGs derived from the VP1 sequence was linked 5′ to the translation initiation site of the VP2 gene (Fig. 14B). The two constructs, SH.BR(3) and SH.BR(2), differed in their reading frames with respect to the final upstream minicistron. They also differed in the degree of overlap of the last minicistron and the translation

initiation site of VP2. The presence of spurious AUGs reduced VP2 production to about 5% of original BR transcripts (Fig. 17). This shows that the seven spurious AUGs role in down regulation is general and not specific for VP1.

CYTOTOXICITY

Introduction of either the entire B19 genome (pYT103 or pYT103c) or only the left side of the genome (pLP) inhibited stable transformation in HeLa cells (Fig. 18, Table 1). The two constructs, pB19SVneo and pB19XmuSVneo, contain almost the full length B19 genome, while pNSSVneo and pNSmuSVneo contain only the left side, coding for the non-structural protein. This inhibition was reversed when a frame shift mutation was introduced in B19 to prevent nonstructural protein expression or production. As a result transformed colonies were observed in HeLa cells.

Figure 17. REDUCED TRANSLATIONAL EFFICIENCY

Reduced translational efficiency of VP2 RNA after addition of VP1 upstream noncoding region. Reactions were terminated at 20 (a) and 60 (b) minutes.

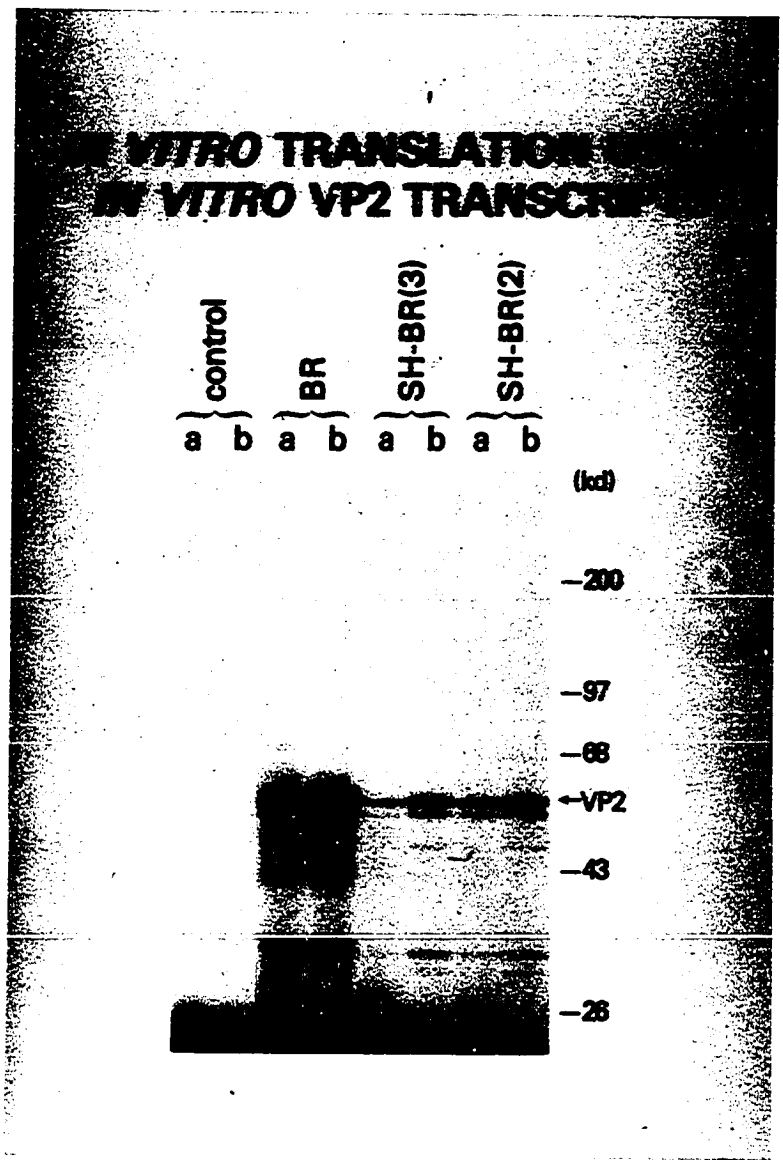

Figure 18. STABLE TRANSFORMATION EXPERIMENT

Stable transformation experiment was done using both B19 and neo^r gene. HeLa cells were transfected with linearized plasmids and selected for neomycin resistance in the presence of G418 for 12 days as described in methods. pB19SVneo was constructed by subcloning of an almost full length pYT103 insert (m.u. 0.17-95) into a pSV2neo vector. pB19XmuSVneo was similar but a frame shift mutation was introduced at m.u. 8. Photographs of the dishes containing transformed colonies, stained with Giemsa, are shown below the respective plasmids.

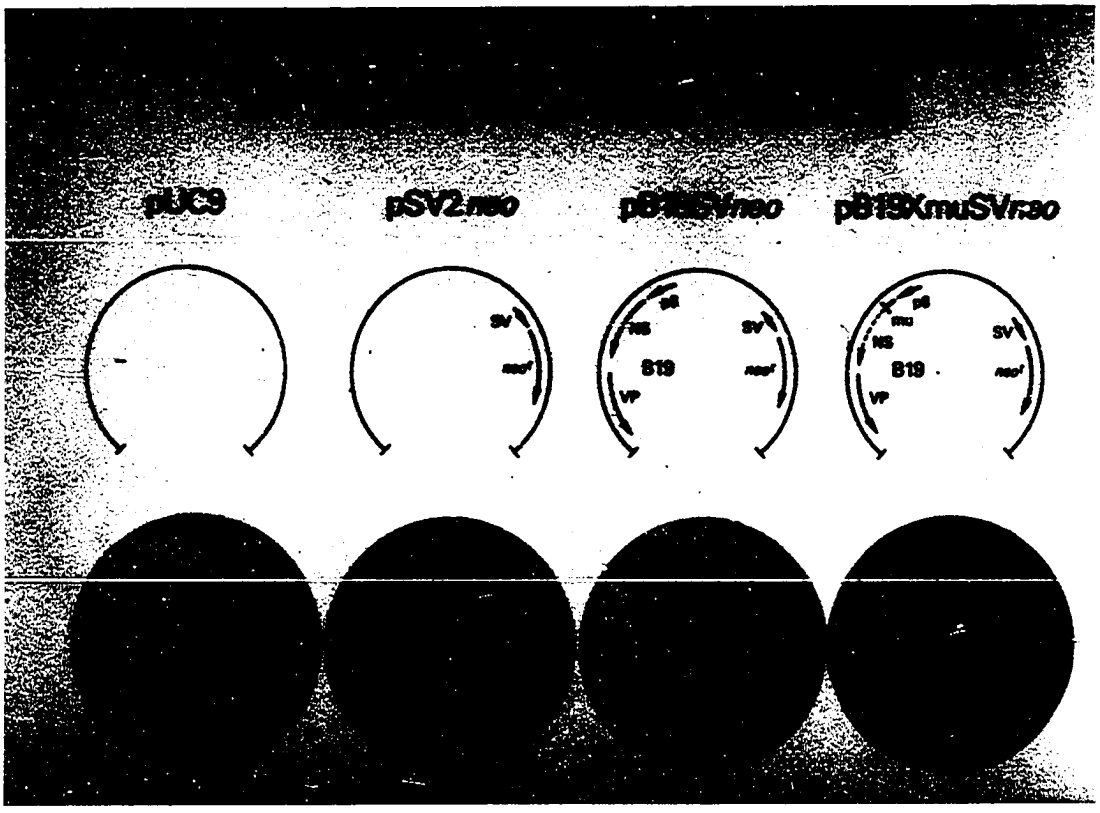

DISCUSSION

The discussion has been divided into into several sub-sections to provide a better understanding of these studies.

TRANSCRIPTION MAP

The B19 parvovirus shares many common features with other parvoviruses. The patterns of RNA transcription for defective (adeno-associated virus) and autonomous parvoviruses are very similar (40, Fig. 19). The B19 structural and capsid proteins are encoded by the right half of the genome, and at least one of the B19 non-capsid proteins by the left half of the genome just as in other parvoviruses. Parvoviruses have a very limited genome length which forces them to use several methods to increase the coding potential of their 5 kilobases of nucleotides. For enhancing this potential they utilize mechanisms which include a pattern of overlapping RNA transcription from extensive utilization of all three reading frames and the generation of multiple RNAs by splicing. An example of these mechanisms is the complex B19 transcription map. The total number of transcripts has ranged from 3-4 for autonomous rodent parvoviruses (34, 41, 42) to 6 for adeno-associated virus-2 (36). The use of alternate nearby splice donor and acceptor sites can generate larger number of transcripts, without apparent size differences, which are usually detected only after cDNA cloning (34,41). In this study at least nine B19 transcripts were identified in RNA extracted from infected erythroid cells. Another full length transcript was suggested on some S1 nuclease analytical gels.

Figure 19. COMPARISION OF TRANSCRIPTION MAP OF B19

The transcription map of B19 is shown rearranged with the maps of AAV2 and MVM. Solid vertical strokes indicate functional and dotted strokes indicate non-functional TATA and AATAAA sequences. A variant polyadenylation signal is indicated in parentheses.

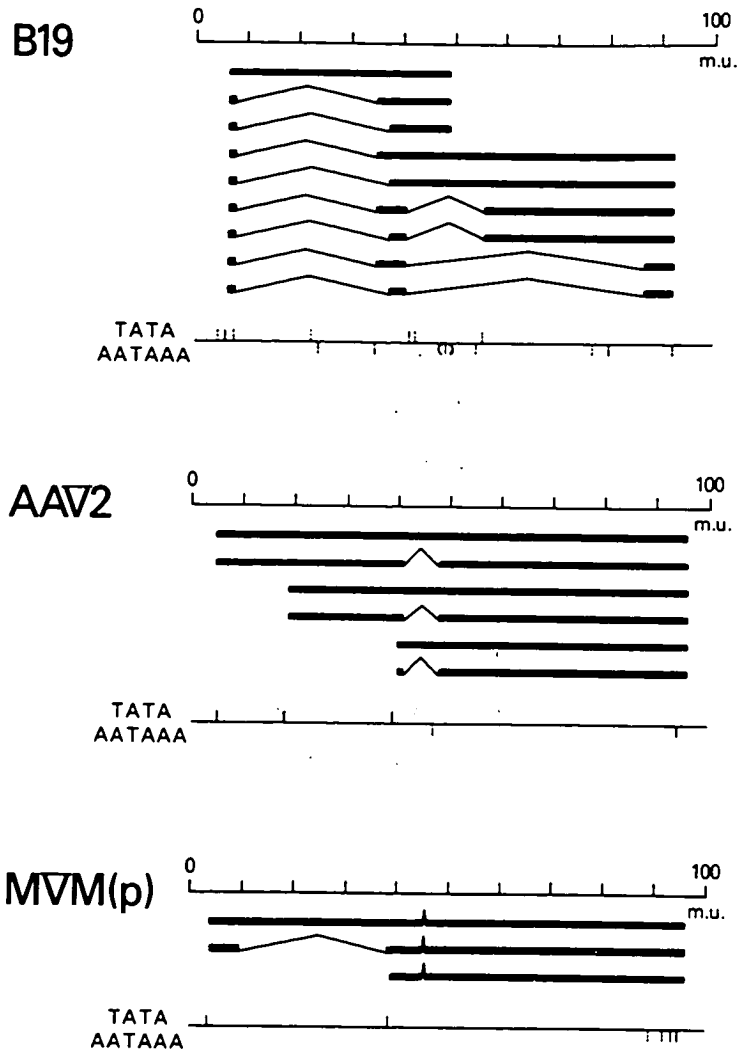

The genomic organization of adeno-associated virus and minute virus of mice is characterized by the presence of two classes of overlapping RNA transcripts - one spliced and the other unspliced (40, Fig. 19). B19 shows such a trio of spliced and unspliced RNAs from the left half of the genome (b, e, f). There are other transcripts which are of almost B19 genome length. These are in pairs and are composed of RNAs with a single long left side intron (a, a'), the left side intron and a short right side intron (c, d), and the left side intron and an even longer right side intron (g, h). These long introns are associated for 8 of 9 RNAs with leader sequences of about 60 bases.

The autonomous parvoviruses have two promoters - one at the left side of the genome (P4-5) for the non-capsid proteins and one in the middle (P38-40) for the capsid proteins. AAV2 has three functional promoter sites (P5, P19, P40). B19 has TATA sequences at map units 5-8, 23, 42-43, and 55. Based on the position of a downstream ATG in an open reading frame, the fourth region, at map unit 55, was thought to be responsible for transcription of the major capsid protein mRNA (21). This study revealed that except for the far left side TATA boxes, all the other promoter regions were located within transcription units. The transcription map showed that all B19 transcripts started at a single far left side promoter located at map unit 6 (P6). This was confirmed by the transient CAT expression assays where only the left side promoter was found to be functionally active. An

internal promoter could not be demonstrated even within erythroid cells.

The nucleotide sequence of B19 showed several possible polyadenylation signals (AATAAA), at map units 24, 35, 54, 77, 80, and 92 (21). Three of the nine B19 transcripts appeared to terminate in the middle of the genome. An unpredicted and unusual polyadenylation signal at map unit 49 (ATTAAA or AATAAC) may have been used by these transcripts. These unusual sequences have rarely been reported as a polyadenylation signal for eukaryotic genes (6, 43) and associated with tissue specificity (44). ATTAAA has been used in 12% of the transcripts while AATAAC in 1% of the transcripts. Their functional character has been suggested by experiments in HeLa cells. HeLa cells were transfected with a plasmid containing sequences from the left side of the B19 genome (map units 0-53), which excludes the conventional polyadenylation signals from the right side of the genome. The same size polyadenylated transcripts, corresponding to b, e, and f, were detected as in cells transfected with full length pYT103 plasmid.

A few protein products of B19 have been identified. The two capsid proteins of 58 and 84 kd (VP2 and VP1) are produced in infected human erythroid bone marrow cells in culture (39). These proteins are also present in virions and in infected human fetal tissue (38, 45). These two capsid proteins compare with structural proteins of other parvoviruses in size and abundance. They are encoded by RNA transcripts from the right side of the B19 genome. The c and d transcripts code for the 58 kd protein while a and a' transcripts code for the less abundant 84 kd

protein. Furthermore, the major non-capsid protein of 77 kd (39) was encoded by transcript b, as determined by promoter deletion and frame shift mutation experiments (Shimada et al, manuscript in preparation). Several B19 RNA transcripts, such as e and f, have no known function.

The coding capacity for several abundant transcripts (e,f,g, and h) is quite limited. It is plausible that they might be coding for undetected, small proteins. That these RNAs might be originating from defective interfering particles (46) is improbable for several reasons. These include that there is no evidence for significant amounts of B19 DNA of other than full genomic length in infected cells (19) and parvovirus defective particles contain large internal deletions (46). These RNAs might have regulatory functions similiar, for example, to adeno-associated virus RNA which increases translation by preventing inactivation of eukaryotic initiation factor 2 (47), or similiar to U1-U6 small nuclear RNAs, which are required for in vitro splicing (48). However, no significant homology was detected between the appropriate regions of the B19 genome spanning nucleotides 1910-2655 and either the human U1 gene or the 5′ end of the VAII adenovirus 5 gene. The U1 gene demonstrated 40% homology by alignment but over many short sequences. On the other hand, only 20% homology was observed with the VAII gene. Both U1 and VA11 were done using Microgenie II.

The nucleotide sequence of B19 has been subjected to a computer analysis. This analysis showed that B19 shared properties with both major genera of Parvoviridae, but that B19

was as separate evolutionarily from autonomous rodent and non pathogenic human AAV as these viruses are from each other (21). For example, B19 shares similarity of its 5′ and 3′ terminal hairpin structures like AAV although it behaves as an autonomous virus in culture (15, 35). Also, both B19 and AAV lack the conserved regions of the right open reading frame common to autonomous parvoviruses (21, 49). This study shows that the transcription map of B19 also diverges significantly from the maps of both defective and autonomous parvoviruses.

The amount of RNAs produced in B19 are regulated. B19 transcript abundance cannot be regulated by differential promoter strength or trans-activation by non-capsid proteins of one of several promoters since it has only a single functional promoter. In other parvoviruses, use of alternate splicing patterns may regulate the differential expression of capsid and non-capsid proteins (40). B19 must rely on splicing events, pausing or termination in the middle of transcription, or polyadenylation signal recognition to control the quantity of the RNAs produced.

OVERLAPPING TRANSCPIPTS

Once the complex transcription map of the B19 parvovirus was established, the next step was to map overlapping transcripts. Overlapping transcription allows a single DNA sequence to encode for multiple proteins, and RNA splicing can increase the number of protein products from a single area of the genome.

RNA size is usually determined by S1 nuclease digestion of RNA-DNA hybrids followed by neutral gel analysis. Alkaline

hydrolysis of RNA within S1 protected RNA-DNA fragments reveal exon size. Exonuclease VII was employed to determine the size of the intervening sequences in the genome. Exonuclease VII analysis of the model RNAs (BS, NBdel, and NAdel) produced similiar 1.9 kb bands for each species because this enzyme does not digest the loop fragment of DNA after DNA-RNA hybridization. The protected fragment therefore includes the introns as well as the exons. S1 analysis determines the size of individual exons in a mixture of unknown RNA molecules. Exonuclease VII analysis shows the size of the RNA exon plus intron but does not help in localizing the position of the exons. In a case of overlapping transcripts with the same initiation and termination sites, all RNA molecules will appear of the same size. This is shown in Fig. 20.

If the RNA-DNA hybrids are preserved their relative electrophoretic mobilities will be different under neutral conditions after exonuclease VII digestion. The bands will separate due to differences in secondary structure among the molecules (Fig. 21). Thus, BS, NBdel and NAdel had different mobilities on neutral gel electrophoresis and the three species separated as three bands when the mixture was applied (Fig. 22). Further, the single spot for the BS RNA (Fig. 13A) was consistent with the same mobility of the protected fragment in the form of an RNA-DNA hybrid and as the probe DNA molecule after alkaline hydrolysis. The mixture of the RNAs was resolved into three bands on two dimensional gels (Fig. 13B). This method thus permits resolution of different transcripts from the same transcription unit.

Figure 20. DETERMINATION OF EXON + INTRON SIZE

Determination of exon plus intron size by exonuclease VII alkaline gel analysis.

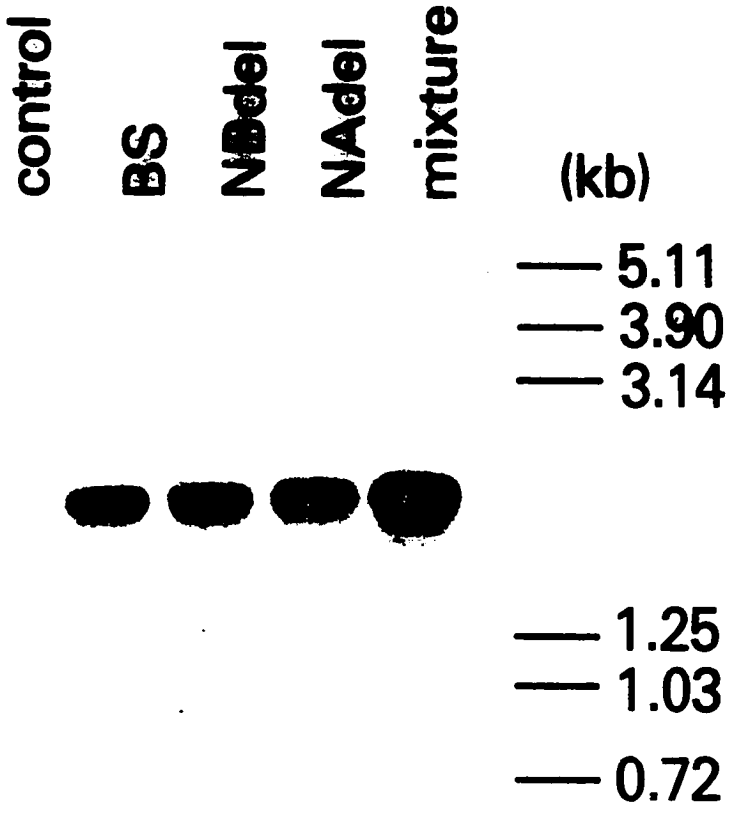

Figure 21. SCHEME OF EXONUCLEASE VII DIGESTION

Alkaline hydrolysis of RNA in the RNA-DNA hybrids after exonuclease VII digestion results in a single band on electrophoresis due to the equivalent size of the remaining DNA probe. In contrast, the protected hybrids will have different apparent molecular weights on electrophoresis due to marked shape differences from the unpaired looped out DNA at the site of the intron removal.

Figure 21.

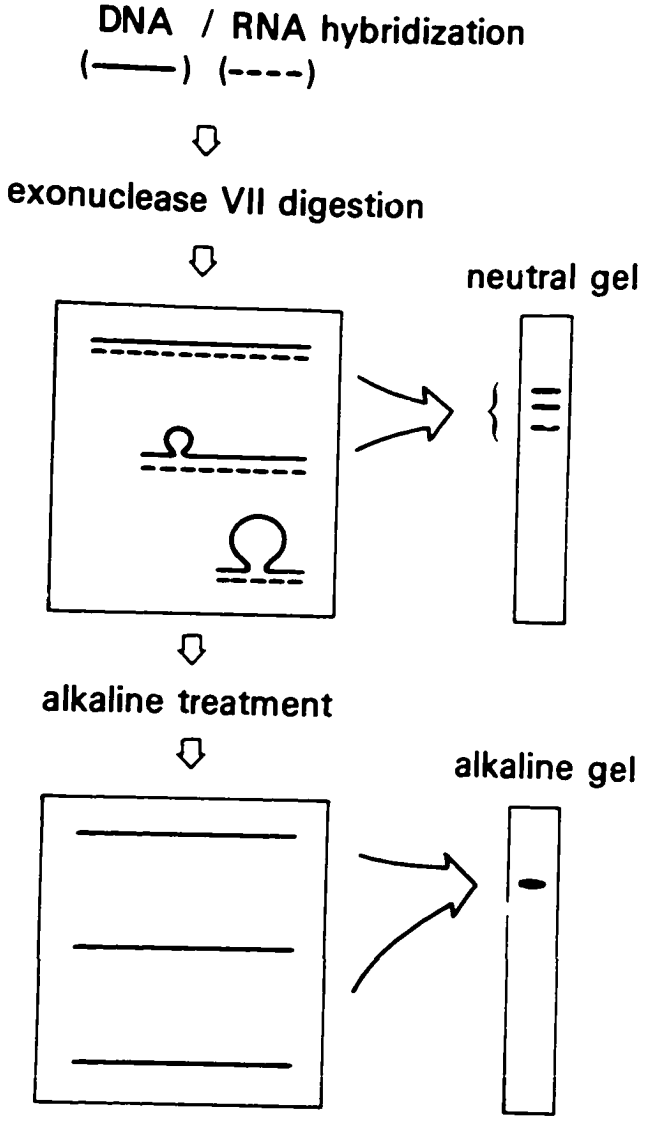

Figure 22. MOBILITY OF RNA-DNA HYBRIDS

Mobility of the exonuclease VII protected RNA-DNA hybrids in neutral gel electrophoresis.

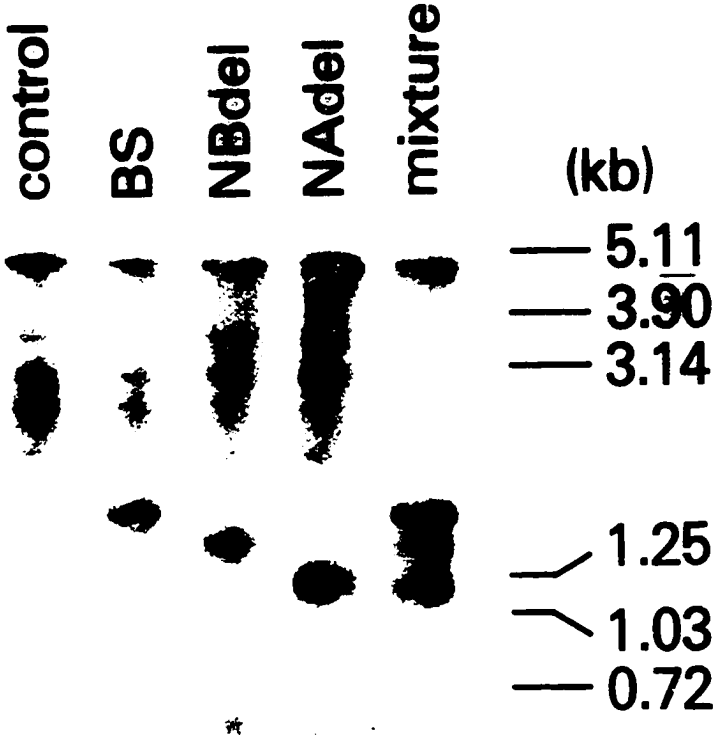

TRANSLATIONAL REGULATION

There is more VP2 than VP1 RNA in infected cells. However, the 5:1 difference in the transcript quantities is not enough to explain the very large amounts of VP2 protein production compared to VP1 (30:1). The data shows that VP2 is translated in vitro much more efficiently than VP1 from synthetic RNAs of native sequence. This is probably due to the suppression of VP1 translation and may, in part, be caused by the presence of multiple spurious AUG codons in a region upstream of the VP1 translation initiation site. This region is removed by splicing during the processing of VP2 RNA.

It has been documented that 40S ribosomal subunits bind at the capped 5′ end and scan the mRNA sequence until an AUG codon is reached (51). The stimulatory effect of the m^7G cap and the inability of the ribosomes to bind to circular mRNAs point to end dependent mechanisms. The importance of position in defining the functional initiation site was shown by manipulating a cloned preproinsulin gene to produce a mRNA in which the ribosome binding site (i.e. an ATG initiator codon and flanking sequence) was tandemly reiterated: ribosomes initiated exclusively at the 5′ proximal copy in the tandem array (63). Inspection of sequences near the 5′ ends of eukaryotic mRNAs provide evidence that might be interpreted for or against the scanning hypothesis. In 90% of the mRNAs examined, there is no extraneous AUG triplets upstream of the functional initiation codon. This finding is rationalized by the scanning model. However, 5-10% of eukaryotic mRNAs have AUG triplet(s) upstream of a known initiation site for

protein synthesis. In such mRNAs, the upstream AUG triplets occur in a context different from the conserved pattern of nucleotides around functional initiation codons. This difference inspired a modified version of the scanning model.

The position and context of the real initiation codon influence translational efficiency in the modified scanning model of translation (51, 52). The 40S ribosomal subunit binds to the capped 5' end of the mRNA and moves along the strand until it reaches an AUG codon. If the AUG is in a favorable context, 60S coupling and protein synthesis occur. If the AUG is not in a favorable context, some of the 40S subunits will continue to migrate along the RNA strand. This is known as leaky scanning. The efficiency of translation from the downstream true initiation site is reduced by upstream spurious AUG codons. If the termination codons are present in-frame following spurious AUG codons, minicistrons are created and reinitiation may occur. This reduces the efficiency of translation from the authentic initiation site. In B19 parvovirus, the region immediately upstream of the VP1 initiation site contains five such minicistrons. Thus, mainly reinitiation rather than leaky scanning probably leads to reduction in the efficiency of VP1 translation. Since the VP1 initiation site is not in a completely optimal context, leaky scanning through it could result in production of VP2 protein from the next downstream AUG codon. Some VP2 protein would then be a byproduct from translation of the VP1 RNA. By computer analysis of secondary RNA structure, the region upstream of VP1 does not contain a stable stem and loop

structure, which could represent another mechanism of down regulation of translation (52, 53, 54).

Thus, the low concentration of VP1 compared to VP2 in B19 parvovirus infected cells is probably due to at least three factors:

1. Production of less VP1 RNA;
2. Translational suppression by upstream multiple spurious AUG codons;
3. Suboptimal contextual sequence for the initiation codon.

The first one is transcriptional while the other two are translational factors.

Some minicistrons are known to produce peptide products. For a yeast gene (CPA1), encoding the glutaminase subunit of carbomoyl-phosphate synthetase, the peptide product of the upstream minicistron was shown to be essential for the repression of CPA1 expression by arginine (55). For SV40, a peptide product of a minicistron without a known function has been identified in infected cells. However, we did not detect a polypeptide product of minicistrons located upstream of the B19 parvovirus VP1 gene. We ran an 8% and 15% polyacrylamide gels with low ^{14}C-labeled protein molecular weight markers. For translation of the proteins we used both wheat germ nuclease and rabbit reticulocyte nuclease. No small polypeptides were detected on either gels. There was no evidence for a trans-acting factor in mixing experiments. Some oncogenes and genes for hormones, hormone receptors, lymphokines, and coagulation proteins have been found to contain upstream minicistrons (56). This finding had been

based on sequence analysis of eukaryotic genes. Spurious upstream AUGs may represent a general and important regulatory mechanism in protein production, especially for the down regulation of protein products that might be harmful in high concentration. However, there are only a few experimentally verified biological examples. For simian virus 40, naturally occurring short RNA species are incorporated into larger polyribosomes that is the predominant and the longer wild type RNA, perhaps reflecting more efficient translational efficiency with removal of upstream AUG codons (57).

CYTOTOXICITY

A variety of possible functions have been assigned to the nonstructural proteins of parvoviruses. In adenoassociated virus deletion of the left side genes stops viral DNA synthesis. These genes are probably essential for viral replication ("rep") function. However, more limited deletions of the left side of the viral genome can have positive as well as negative effects on virus production, which to some extent depend on the host cell (36,61). The nonstructural protein has a trans-activating effect on the capsid protein promoter for a rat parvovirus (61). Cells, transfected with selectable marker genes and the B19 nonstructural genes, did not show transformation to antibiotic resistance. This is probably due to nonstructural protein blocking cell proliferation or effecting cell death.

The B19 nonstructural protein is localized to the nuclei of infected cells (39), where it could affect host cell DNA

replication. We failed in our attempts to discriminate a cytostatic from cytotoxic effect using cells transfected with the B19 nonstructural gene that was linked to the mouse mammary tumor virus promoter, followed by steroid induction. Inability to achieve inducible expression by nonstructural gene has been reported for the H1 rat parvovirus. Virus propagation is probably slowed by a strong inhibitory effect of nonstructural protein on host cell mechanisms. For hematopoietic cells a block on cell proliferation is functionally equivalent to cytotoxicity.

SIGNIFICANCE

The major achievement of this study is that we were able to establish the transcription map of the B19 (human) pathogenic parvovirus. B19 transcription map has unusual features in comparison with that of other parvoviruses. At least nine overlapping B19 transcripts were identified and all, except one, contained large introns. B19 differed from other parvoviruses in some important aspects. In B19 all transcripts initiated at a strong left side promoter and had no functional internal promoter. Short 5′ leader sequences were present and very large introns for RNA were encoded by the right side of the genome. Unlike other parvoviruses, two separate transcription termination sites were detected in B19. Some of the overlapping transcripts of B19 had the same initiation and termination sites but contained introns of differing sizes. Two dimensional electrophoresis was employed for the exonuclease VII analysis of these transcripts. Single bands were resolved into components of

appropriate sizes. Further, the production and regulation of capsid proteins by overlapping transcripts was studied by investigating into the upstream ATG codons. These codons can cause leaky scanning which, in turn, can lead to a decrease in the efficiency of protein production in B19. However, reinitiation rather than leaky scanning leads to a reduction in the efficiency of VP1 translation. Finally, we attempted to demonstrate that the B19 non-structural protein of 77 kd is cytotoxic to the HeLa cells when selection was done in the presence of the antibiotic G418.

BIBLIOGRAPHY

1. Mathews,R.E.F. Classification and nomenclature of viruses. Intervirology, 1982, vol. 17, p. 72-75.

2. Cossart,Y.E., Field,A.M., Cant,B., and Widdows,D. Parvovirus-like particles in human sera. Lancet, 1974, vol. 1, p. 72-73.

3. Vandervelde,E.M., Goffin,C., Megson,B., Mahmood,N., Porter,A., and Cossart,Y.E. User's guide to some new tests for hepatitis-B antigen. Lancet, 1974, vol. 2, p. 1066-1068.

4. Edwards,J.M.B., Kessel,I., Gardner,S.D., Eaton,B.R., Pollock,T.M., Fleck,D.C., Gibson,P., Woodroof,M., and Porter,A.D. A search for characteristic illness in children with serological evidence of viral or toxoplasma infection. J.Infect., 1981, vol. 3, p. 316-323.

5. Shneerson,J.M., Mortimer,P.P., and Vandervelde,E.M. Febrile illness due to a parvovirus. Brit.Med.J., 1980, vol. 2, p. 1580.

6. Anderson,M.J., Davis,L.R., Hodgson,J., Jones,S.E., Murtaza,L., Pattison,J.R., Strond,C.E., and White,J.M. Occurrence of infection with a parvovirus-like agent in children with sickle-cell anemia during a two-year period. J.Clin.Path., 1982, vol. 35, p. 744-749.

7. Kelleher,J.H., Luban,N.L.C., Mortimer,P.P., and Kamimura,T. The human serum "parvovirus". A specific cause of aplastic crises in hereditary spherocytosis. J.Pediatr., 1983, vol. 102, p. 720-722.

8. Summer,J., Jones,S.E., and Anderson,M.J. Characterization of

the agent of erthrocyte aplasia as a human parvovirus. J.Gen.Virol., 1984, vol. 64, p. 2527-2532.

9. Anderson,M.J., Pattison,J.R., and Young,N.S. Pathogenesis of parvovirus-induced diseases in humans. Concepts in Viral Pathogenesis II. Notkins,A.L., and Oldstone,M.B.A. (eds.), Springer Verlag New York Inc., New York. 1986, vol. 2, p. 261-268.

10. Anderson,M.J., Lewis,E., Kidd,I.M., Hall,S.M., and Cohen,B.J. An outbreak of erythema infectiosum associated with human parvovirus infection. J.Hyg.(camb), 1984, vol. 93, p. 85-93.

11. Pattison,J.R., Jones,S.E., Hodgson,J., Davis,L.R., White,J.M., Strand,C.E., and Murtaza,L. Parvovirus infection and hypoplastic crisis in sickle cell anaemia. Lancet, 1982, vol. 1, p. 664-665.

12. Serjeant,G.R., Mason,K., Topley,J.M., Serjeant,B.M., Pattison,J.R., Jones,S.E., and Mohammed,R. Outbreak of aplastic crisis in sickle cell anaemia associated with parvovirus-like agent. Lancet, 1981, vol. 2, p. 595-597.

13. Chourba,T.L., Coccia,P., Holman,R.C., Tattersal,P., Anderson,L.J., Sudman,J., Young,N.S., Kureyznski,E., Palmer,E., Jason,J., and Evatt,B. The role of parvovirus B19 in aplastic crisis and erythema infectiosum (fifth disease). J.Infect.Dis., 1986, vol. 154, p. 383-393.

14. Saarinen,U.M., Chourba,T.L., Tattersal,P., Young,N.S., Anderson,L.J., and Coccia,P. Human parvovirus B19-induced epidemic acute red cell aplasia in patients with hereditary

hemolytic anemia. Blood, 1986, vol. 67, p. 1411-1417.

15. Young,N.S., Mortimer,P.P., Moore,J.G., and Humphries,R.K. Characterization of a virus that causes transient aplastic crisis. J.Clin.Invest., 1984, vol. 73, p. 224-230.

16. Berns,K.I., Cheung,A.K.M., Ostrove,J.M., and Lewis,M. Adeno-associated virus latent infection. In Mahy,M.W.J., Muison,A.C., and Darby,C.K. (eds.), Virus Persistence, Cambridge University Press, Cambridge. 1982, p. 249.

17. Knott,P.D., Welply,G.A.C., and Anderson,M.J. Serologically proven intrauterine infection with parvovirus. Br.Med.J., 1984, vol. 289, p. 1660.

18. Brown,T., Anand,A., Ritchie,L.E., Clewley,J.P., and Reid,T.M.S. Intrauterine human parvovirus infection and hydrops fetalis. Lancet, 1984, vol. 2, p. 1033-1034.

19. Ozawa,K., Kurtzman,G., and Young,N. Replication of the B19 Parvovirus in human bone marrow cell cultures. Science, 1986, vol. 233, p. 883-886.

20. Harper,M.E., Marselle,L.M., Gallo,R.C., and Wong-Staal,F. Detection of lymphocytes expressing human T-lymphotrophic virus type III in lymph nodes and peripheral blood from infected individuals by in-situ hybridization. Proc.Nat.Acad.Sci., U.S.A., 1986, vol. 83, p. 772-776.

21. Shade,R.O., Blundell,M.C., Cotmore,S.F., Tattersal,P., and Astell,C.R. Nucleotide sequence and genome organization of human parvovirus B19 isolated from the serum of a child during aplastic crisis. J.Virol., 1986, vol. 58, p. 921-936.

22. Werner,D., Chemla,Y., and Herzber,M. Isolation of poly(A)+

RNA by paper affinity chromatography. Anal.Biochem., 1984, vol. 141, p. 329-336.

23. Maniatis,T., Fritch,R.F., and Sambrook,J. Molecular Cloning. Cold Spring Harbor, New York, 1982.

24. Berk,A.J., and Sharp,P.A. Sizing and mapping of early adenovirus mRNAs by gel electrophoresis of S1 endonuclease digested hybrids. Cell, 1977, vol. 12, p. 721-732.

25. Favaloro,J., Treisman,R., and Kamen,R. Transcription maps of polyomoa virus-specific RNA analysis by two dimensional nuclease S1 gel mapping. Meth.Enzymol., 1980, vol. 65, p. 718-749.

26. Cotmore,S.R., and Tattersal,P. Characterization of molecular cloning of a human parvovirus genome. Science, 1984, vol. 226, p. 1161-1165.

27. Sharp,P.A., Berk,A.J., and Berget,S.M. Transcription maps of adenovirus. Meth.Enzymol., 1980, vol. 65, p. 750-768.

28. Melton,D.A., Kreig,P.A., Rebagliati,M.R., Maniatis,T., Zinn,K., and Green,M.R. Efficient in vitro synthesis of biologically active RNA and RNA hybridization probes from plasmids containing a bacteriophage SP6 promoter. Nucl.Acids Res., 1984, vol. 12, p. 7035-7056.

29. Treisman,R., Proudfoot,N.J., Shander,M., and Maniatis,T. A single-base change at a splice site in a β-thalassemic gene causes abnormal RNA splicing. Cell, 1982, vol. 29, p. 903-911.

30. Potter,H., Weir,L., and Leder,P. Enhancer-dependent expression of human k immunoglobulin genes introduced into

mouse pre-B lymphocytes by electroporation. Proc.Nat.Acad.Sci. U.S.A., 1984, vol. 81, p. 7161-7165.

31. Gorman,G.M., Moffat,L.F., and Howard,B.H. Recombinant genomes which express chloramphenicol acetyltransferase in mammalian cells. Molec.Cell.Biol., 1982, vol. 2, p. 1044-1051.

32. Davis,L.G., Dibner,M.E., and Battey,J.F. Basic Methods in Molecular Biology. Elsevier Science Publishing Co.,Inc., New York, 1986, p. 306-310.

33. Goding,J.W. (ed.), Monoclonal Antibodies: Principles and Practices. Academic Press, New York, 1983.

34. Jongeneel,C.V., Sahli,R., McMaster,G.K., and Hirt,B. A precise map of splice junctions in the mRNAs of minute virus of mice, an autonomous parvovirus. J.Virol., 1986, vol. 59, p. 564-573.

35. Ozawa,K., Kurtzman,G., and Young,N. Productive infection by B19 Parvovirus of human erythroid bone marrow cells in vitro. Blood, 1987, vol. 70, p. 384-391.

36. Tratschin,J.D., Tal,J., and Carter,B.J. Negative and positive regulation in <u>trans</u> of gene expression from adeno-associated virus vectors in mammalian cells by a viral rep gene product. Molec.Cell.Biol., 1986, vol. 6, p. 2884-2894.

37. Kozak,M. Compilation and analysis of sequence upstream from the traditional start site in eukaryotic mRNAs. Nucl.Acids Res., 1984, vol. 12, p. 857-872.

38. Cotmore,S.F., McKie,V.C., Anderson,L.J., Astell,C.R., and

Tattersal,P. Identification of the major structural and non-structural proteins encoded by human parvovirus B19 and mapping of their genes by procaryotic expression of isolated fragments. J.Virol., 1986, vol. 60, p. 548-557.

39. Ozawa,K., and Young,N. Characterization of capsid and non capsid proteins of B19 Parvovirus propagated in human erythroid bone marrow cell cultures. J.Virol., 1987, vol. 61, p. 2627-2630.

40. Carter,B.J., Laughlin,C.A., and Marcus-Sekura,C.J. Parvovirus transcription. The Parvoviruses, Berns,K.I. (ed.), Plenum Publishing Corp., New York, 1984, p. 153-208.

41. Morgan,W.R., and Ward,D.C. Three splicing patterns are used to excise the small intron common to all minute virus of mice RNAs. J.Virol., 1986, vol. 60, p. 1170-1174.

42. Lebovitz,R.M., and Roeder,R.G. Parvovirus H-1 expression: mapping of the abundant cytoplasmic transcripts and identification of promoter sites and overlapping transcription units. J.Virol., 1986, vol. 58, p. 271-280.

43. Wickens,M., and Stephenson,P. Role of the conserved AAUAAA sequence: four AAUAAA point mutants prevent messenger RNA 3' end formation. Science, 1984, vol. 226, p. 1045-1051.

44. Young,R.A., Hagenbuchle,O., and Schibler,U. A single mouse α-amylase gene specifies two different tissue-specific mRNAs. Cell, 1981, vol. 23, p. 451-458.

45. Young,N., and Ozawa,K. Studies of the B19 parvovirus in bone marrow cell culture. Parvoviruses and human diseases, Pattison,J. (ed.), CRC Press, Boca Raton, Florida, 1987,

p. 117-132.

46. Carter,B.J. Variant and defective interfacing parvoviruses. The Parvoviruses, Berns,K.I. (ed.), Plenum Publishing Corp., New York, 1984, p. 209-258.

47. Schneider,R.J., Safer,B., Mumemitsu,S.M., Samuel,C.E., and Shenk,T. Adenovirus VAI RNA prevents phosphorylation of the eukaryotic expression factor 2 α-subunit subsequent to infection. Proc.Nat.Acad.Sci. U.S.A., 1985, vol. 82, p. 4321-4325.

48. Berget,S.M., and Robberson,B.L. U1, U2, and U4/U6 small nuclear ribonucleoproteins are required for in vitro splicing but not polyadenylation. Cell, 1986, vol. 46, p. 691-696.

49. Chen,K.C., Shull,B.C., Moses,E.A., Lederman,M., Stout,E.R., and Bates,R.C. Complete nucleotide sequence and genome organization of bovine parvovirus. J.Virol., 1986, vol. 60, p. 1085-1097.

50. Siegl,G. Biology and pathogenicity of autonomous parvoviruses. The Parvoviruses, Berns,K.I. (ed.), Plenum Publishing Corp., New York, 1984, p. 297-362.

51. Kozak,M. Point mutations define a sequence flanking the AUG initiation codon that modulates translation by eukaryotic ribosomes. Cell, 1986, vol. 44, p. 283-292.

52. Kozak,M. Regulation of protein synthesis in virus-infected animal cells. Adv.Virus Res., 1986, vol. 31, p. 229-292.

53. Pelletier,J., and Sonnenberg,N. Insertion mutagenesis to increase secondary structure within the 5' noncoding region

of a eukaryotic mRNA reduces translational efficiency. Cell, 1985, vol. 40, p. 515-526.

54. Kozak,M. Influence of mRNA secondary structure on initiation by eukaryotic ribosomes. Proc.Nat.Acad.Sci. U.S.A., 1986, vol. 83, p. 2850-2854.

55. Werner,M., Feller,A., Hessonguy,F., and Pierard,A. The leader peptide of the yeast gene CPA1 is essential for the translational repression of its expression. Cell, 1987, vol. 49, p. 805-813.

56. Kozak,M. Bifunctional messenger RNAs in eukaryotes. Cell, 1986, vol. 47, p. 481-483.

57. Barkan,A., and Mertz,J.E. The number of ribosomes on Simian Virus 40 late 16S mRNA is determined in part by the nucleotide sequence of its leader. Mol.Cell.Biol., 1984, vol. 4, p. 813-816.

58. Mueller,P.P., and Hinnebusch,A.G. Multiple upstream AUG codon mediate translational control of GCN4. Cell, 1986, vol. 45, p. 201-207.

59. Tzamarias,D., Alexandraki,D., and Thireos,G. Multiple cis-acting elements modulate the translational efficiency of GCN4 mRNA in yeast. Proc.Nat.Acad.Sci. U.S.A., 1986, vol. 83, p. 4849-4853.

60. Khalili,K., Brady,J., and Khoury,G. Translational regulation of SV40 early mRNA defines a new viral protein. Cell, 1987, vol. 48, p. 639-645.

61. Labow,M.A., Hermonant,P.L., and Berns,K.I. Positive and negative autoregulation of the AAV type 2 genome. J.Virol.,

1986, vol. 60, p. 251-258.

62. Rhode,S.L.III. Trans-activation of parvovirus P_{38} promoter by the 76K noncapsid protein. J.Virol., 1985, vol. 55, p. 886-889.

63. Kozak,M. Translation of insulin related polypeptides from mRNAs with tandemly reiterated copies of the ribosome binding site. Cell, 1983, vol. 34, p. 971-978.

APPENDIX

The nucleotide sequence of the B19 (human) pathogenic parvovirus is included in this appendix. The sequence was obtained from the MICROGENIE computer program.

B19 PARVOVIRUS NUCLEOTIDE SEQUENCE

```
        10          20          30          40          50          60
GAATTCCGCC AAATCAGATG CCGCCGGTCG CCGCCGGATG GCGGGACTTC CGGTACAAGA
        70          80          90         100         110         120
TGGCGGACAA TTACGTCATT TCCTGTGACG TCATTTCCTG TGACGTCACA GGAAATGACG
       130         140         150         160         170         180
TAATTGTCCG CCATCTTGTA CCGGAAGTCC CGCCTACCGG CGGCGACCGG CGGCATCTGA
       190         200         210         220         230         240
TTTGGTGTCT TCTTTTAAAT TTTAGCGGGC TTTTTTCCCG CCTTATGCAA ATGGGCAGCC
       250         260         270         280         290         300
ATTTTAAGTG TTTTACTATA ATTTTATTGG TTAGTTTTGT AACGGTTAAA ATGGGCGGAG
       310         320         330         340         350         360
CGTAGGCGGG GACTACAGTA TATATAGCAC GGTACTGCCG CAGCTCTTTC TTTCTGGGCT
       370         380         390         400         410         420
GCTTTTTCCT GGACTTTCTT GCTGTTTTTT GTGAGCTAAC TAACAGGTAT TTATACTACT
       430         440         450         460         470         480
TGTTAACATC CTAACATGGA GCTATTTAGA GGGGTGCTTC AAGTTTCTTC TAATGTTCTA
       490         500         510         520         530         540
GACTGTGCTA ACGATAACTG GTGGTGCTCT TTACTGGATT TAGACACTTC TGACTGGGAA
       550         560         570         580         590         600
CCACTAACTC ATACTAACAG ACTAATGGCA ATATACTTAA GCAGTGTGGC TTCTAAGCTT
       610         620         630         640         650         660
GACTTTACCG GGGGGCCACT AGCAGGGTGC TTGTACTTTT TTCAAGTAGA ATGTAACAAA
       670         680         690         700         710         720
TTTGAAGAAG GCTATCATAT TCATGTGGTT ACTGGGGGGC CAGGGTTAAA CCCCAGAAAC
       730         740         750         760         770         780
CTTACAGTGT GTGTAGAGGG GTTATTTAAT AATGTACTTT ATCACCTTGT AACTGAAAAT
```

790 800 810 820 830 840

GTGAAGCTAA AATTTTTGCC AGGAATGACT ACAAAAGGCA AATACTTTAG AGATGGAGAG

850 860 870 880 890 900

CAGTTTATAG AAAACTATTT AATGAAAAAA ATACCTTTAA ATGTTGTATG GTGTGTTACT

910 920 930 940 950 960

AATATTGATG GATATATAGA TACCTGTATT TCTGCTACTT TTAGAAGGGG AGCTTGCCAT

970 980 990 1000 1010 1020

GCCAAGAAAC CCCGCATTAC CACAGCCATA AATGATACTA GTAGTGATGC TGGGGAGTCT

1030 1040 1050 1060 1070 1080

AGCGGCACAG GGGCAGAGGT TGTGCCATTT AATGGGAAGG GAACTAAGGC TAGCATAAAG

1090 1100 1110 1120 1130 1140

TTTCAAACTA TGGTAAACTG GTTGTGTGAA AACAGAGTGT TTACAGAGGA TAAGTGGAAA

1150 1160 1170 1180 1190 1200

CTAGTTGACT TTAACCAGTA CACTTTACTA AGCAGTAGTC ACAGTGGAAG TTTTCAAATT

1210 1220 1230 1240 1250 1260

CAAAGTGCAC TAAAACTAGC AATTTATAAA GCAACTAATT TAGTGCCTAC TAGCACATTT

1270 1280 1290 1300 1310 1320

TTATTGCATA CAGACTTTGA GCAGGTTATG TGTATTAAAG ACAATAAAAT TGTTAAATTG

1330 1340 1350 1360 1370 1380

TTACTTTGTC AAAACTATGA CCCCCTATTG GTGGGGCAGC ATGTGTTAAA GTGGATTGAT

1390 1400 1410 1420 1430 1440

AAAAAATGTG GTAAGAAAAA TACACTGTGG TTTTATGGGC CGCCAAGTAC AGGAAAAACA

1450 1460 1470 1480 1490 1500

AACTTGGCAA TGGCCATTGC TAAAAGTGTT CCAGTATATG GCATGGTTAA CTGGAATAAT

1510 1520 1530 1540 1550 1560

GAAAACTTTC CATTTAATGA TGTAGCAGGA AAAAGCTTGG TGGTCTGGGA TGAAGGTATT

1570 1580 1590 1600 1610 1620

ATTAAGTCTA CAATTGTAGA AGCTGCAAAA GCCATTTTAG GCGGGCAACC CACCAGGGTA

1630 1640 1650 1660 1670 1680

GATCAAAAAA TGCGTGGAAG TGTAGCTGTG CCTGGAGTAC CTGTGGTTAT AACCAGCAAT

1690 1700 1710 1720 1730 1740

GGTGACATTA CTTTTGTTGT AAGCGGGAAC ACTACAACAA CTGTACATGC TAAAGCCTTA

1750 1760 1770 1780 1790 1800

AAAGAGCGCA TGGTAAAGTT AAACTTTACT GTAAGATGCA GCCCTGACAT GGGGTTACTA

1810 1820 1830 1840 1850 1860

ACAGAGGCTG ATGTACAACA GTGGCTTACA TGGTGTAATG CACAAAGCTG GGACCACTAT

1870 1880 1890 1900 1910 1920

GAAAACTGGG CAATAAACTA CACTTTTGAT TTCCCTGGAA TTAATGCAGA TGCCCTCCAC

1930 1940 1950 1960 1970 1980

CCAGACCTCC AAACCACCCC AATTGTCACA GACACCAGTA TCAGCAGCAG TGGTGGTGAA

1990 2000 2010 2020 2030 2040

AGCTCTGAAG AACTCAGTGA AAGCAGCTTT TTTAACCTCA TCACCCCAGG CGCCTGGAAC

2050 2060 2070 2080 2090 2100

ACTGAAACCC CGCGCTCTAG TACGCCCATC CCCGGGACCA GTTCAGGAGA ATCATTTGTC

2110 2120 2130 2140 2150 2160

GGAAGCCCAG TTTCCTCCGA AGTTGTAGCT GCATCGTGGG AAGAAGCCTT CTACACACCT

2170 2180 2190 2200 2210 2220

TTGGCAGACC AGTTTCGTGA ACTGTTAGTT GGGGTTGATT ATGTGTGGGA CGGTGTAACG

2230 2240 2250 2260 2270 2280

GGTTTACCTG TGTGTTGTGT GCAACATATT AACAATAGTG GGGGAGGGTT GGGACTTTGT

2290 2300 2310 2320 2330 2340

CCCCATTGCA TTAATGTAGG GGCTTGGTAT AATGGATGGA AATTTCGAGA ATTTACCCCA

2350 2360 2370 2380 2390 2400

GATTTGGTGC GATGTAGCTG CCATGTGGGA GCTTCTAATC CCTTTTCTGT GCTAACCTGC

2410 2420 2430 2440 2450 2460

AAAAAATGTG CTTACCTGTC TGGATTGCAA AGCTTTGTAG ATTATGAGTA AAAAAAGTGG

2470 2480 2490 2500 2510 2520

CAAATGGTGG GAAAGTGATG ATAAATTTGC TAAAGCTGTG TATCAGCAAT TTGTGGAATT

2530 2540 2550 2560 2570 2580

TTATGAAAAG GTTACTGGAA CAGACTTAGA GCTTATTCAA ATATTAAAAG ATCATTATAA

2590 2600 2610 2620 2630 2640

TATTTCTTTA GATAATCCCC TAGAAAACCC ATCCTCTCTG TTTGACTTAG TTGCTCGTAT

2650 2660 2670 2680 2690 2700

TAAAAATAAC CTTAAAAACT CTCCAGACTT ATATAGTCAT CATTTTCAAA GTCATGGACA

2710 2720 2730 2740 2750 2760

GTTATCTGAC CACCCCCATG CCTTATCATC CAGTAGCAGT CATGCAGAAC CTAGAGGAGA

2770 2780 2790 2800 2810 2820

AAATGCAGTA TTATCTAGTG AAGACTTACA CAAGCCTGGG CAAGTTAGCG TACAACTACC

2830 2840 2850 2860 2870 2880

CGGTACTAAC TATGTTGGGC CTGGCAATGA GCTACAAGCT GGGCCCCCGC AAAGTGCTGT

2890 2900 2910 2920 2930 2940

TGACAGTGCT GCAAGGATTC ATGACTTTAG GTATAGCCAA CTGGCTAAGT TGGGAATAAA

2950 2960 2970 2980 2990 3000

TCCATATACT CATTGGACTG TAGCAGATGA AGAGCTTTTA AAAAATATAA AAAATGAAAC

3010 3020 3030 3040 3050 3060

TGGGTTTCAA GCACAAGTAG TAAAAGACTA CTTTACTTTA AAAGGTGCAG CTGCCCCTGT

3070 3080 3090 3100 3110 3120

GGCCCATTTT CAAGGAAGTT TGCCGGAAGT TCCCGCTTAC AACGCCTCAG AAAAATACCC

3130 3140 3150 3160 3170 3180

AAGCATGACT TCAGTTAATT CTGCAGAAGC CAGCACTGGT GCAGGAGGGG GGGGCAGTAA

3190 3200 3210 3220 3230 3240

TTCTGTCAAA AGCATGTGGA GTGAGGGGGG CACTTTTAGT GCTAACTCTG TAACTTGTAC

3250 3260 3270 3280 3290 3300

ATTTTCCAGA CAGTTTTTAA TTCCATATGA CCCAGAGCAC CATTATAAGG TGTTTTCTCC

3310 3320 3330 3340 3350 3360

CGCAGCGAGT AGCTGCCACA ATGCCAGTGG AAAGGAGGCA AAGGTTTGCA CCATCAGTCC

3370 3380 3390 3400 3410 3420

CATAATGGGA TACTCAACCC CATGGAGATA TTTAGATTTT AATGCTTTAA ATTTATTTTT

3430 3440 3450 3460 3470 3480

TTCACCTTTA GAGTTTCAGC ACTTAATTGA AAATTATGGA AGTATAGCTC CTGATGCTTT

3490 3500 3510 3520 3530 3540

AACTGTAACC ATATCAGAAA TTGCTGTTAA GGATGTTACA GACAAAACTG GAGGGGGGGT

3550 3560 3570 3580 3590 3600

ACAGGTTACT GACAGCACTA CAGGGCGCCT ATGCATGTTA GTAGACCATG AATACAAGTA

3610 3620 3630 3640 3650 3660

CCCATATGTG TTAGGGCAAG GTCAGGATAC TTTAGCCCCA GAACTTCCTA TTTGGGTATA

3670 3680 3690 3700 3710 3720

CTTTCCCCCT CAATATGCTT ACTTAACAGT AGGAGATGTT AACACACAAG GAATTTCTGG

3730 3740 3750 3760 3770 3780

AGACAGCAAA AAATTAGCAA GTGAAGAATC AGCATTTTAT GTTTTGGAAC ACAGTTCTTT

3790 3800 3810 3820 3830 3840

TCAGCTTTTA GGTACAGGAG GTACAGCATC TATGTCTTAT AAGTTTCCTC CAGTGCCCCC

3850 3860 3870 3880 3890 3900

AGAAAATTTA GAGGGCTGCA GTCAACACTT TTATGAAATG TACAATCCCT TATACGGATC

3910 3920 3930 3940 3950 3960

CCGCTTAGGG GTTCCTGACA CATTAGGAGG TGACCCAAAA TTTAGATCTT TAACACATGA

3970 3980 3990 4000 4010 4020

AGACCATGCA ATTCAGCCCC AAAACTTCAT GCCAGGGCCA CTAGTAAACT CAGTGTCTAC

4030 4040 4050 4060 4070 4080

AAAGGAGGGA GACAGCTCTA ATACTGGAGC TGGAAAAGCC TTAACAGGCC TTAGCACAGG

4090 4100 4110 4120 4130 4140

TACCTCTCAA AACACTAGAA TATCCTTACG CCCTGGGCCA GTGTCTCAGC CATACCACCA

4150 4160 4170 4180 4190 4200

CTGGGACACA GATAAATATG TCACAGGAAT AAATGCCATT TCTCATGGTC AGACCACTTA

4210 4220 4230 4240 4250 4260

TGGTAACGCT GAAGACAAAG AGTATCAGCA AGGAGTGGGT AGATTTCCAA ATGAAAAAGA

4270 4280 4290 4300 4310 4320

ACAGCTAAAA CAGTTACAGG GTTTAAACAT GCACACCTAC TTTCCCAATA AAGGAACCCA

4330 4340 4350 4360 4370 4380

GCAATATACA GATCAAATTG AGCGCCCCCT AATGGTGGGT TCTGTATGGA ACAGAAGAGC

4390 4400 4410 4420 4430 4440

CCTTCACTAT GAAAGCCAGC TGTGGAGTAA AATTCCAAAT TTAGATGACA GTTTTAAAAC

4450 4460 4470 4480 4490 4500

TCAGTTTGCA GCCTTAGGAG GATGGGGTTT GCATCAGCCA CCTCCTCAAA TATTTTTAAA

4510 4520 4530 4540 4550 4560

AATATTACCA CAAAGTGGGC CAATTGGAGG TATTAAATCA ATGGGAATTA CTACCTTAGT

4570 4580 4590 4600 4610 4620

TCAGTATGCC GTGGGAATTA TGACAGTAAC TATGACATTT AAATTGGGGC CCCGTAAAGC

4630 4640 4650 4660 4670 4680

TACGGGACGG TGGAATCCTC AACCTGGAGT ATATCCCCCG CACGCAGCAG GTCATTTACC

4690 4700 4710 4720 4730 4740

ATATGTACTA TATGACCCCA CAGCTACAGA TGCAAAACAA CACCACAGAC ATGGATATGA

4750 4760 4770 4780 4790 4800

AAAGCCTGAA GAATTGTGGA CAGCCAAAAG CCGTGTGCAC CCATTGTAAA CACTCCCCAC

4810 4820 4830 4840 4850 4860

CGTGCCTCCA GCCAGGATGC GTAACTAAAC GCCCACCAGT ACCACCCAGA CTGTACCTGC

4870 4880 4890 4900 4910 4920

CCCCTCCTGT ACCTATAAGA CAGCCTAACA CAAAAGATAT AGACAATGTA GAATTTAAGT

4930 4940 4950 4960 4970 4980

ACTTAACCAG ATATGAACAA CATGTTATTA GAATGTTAAG ATTGTGTAAT ATGTATCAAA

4990 5000 5010 5020 5030 5040

ATTTAGAAAA ATAAACATTT GTTGTGGTTA AAAAATTATG TTGTTGCGCT TTAAAAATTT

5050 5060 5070 5080 5090 5100

AAAAGAAGAC ACCAAATCAG ATGCCGCCGG TCGGCCGGTA GGCGGGACTT CCGGTACAAG

5110

ATGGCGGAAT TC

AUTOBIOGRAPHICAL STATEMENT

Mr. Jamshed Ayub was born on October 20, 1955 in the city of Agra in India. His father, Mohammed Ayub, was a businessman while his mother, Rashida Khatoon, was a housewife. He married Bushra Seema Omer on July 4, 1982 in Karachi, Pakistan. He has a daughter, Suniah Seema Ayub, who was born on January 12, 1987.

Mr. Ayub graduated from Aligarh Muslim University in Aligarh, India in 1975 with a Bachelor of Science (Honors) in Chemistry. He recieved his Master of Science in Biochemistry in 1977 from the same university. He then left India to pursue higher studies in the United States of America. He joined Old Dominion University in 1979 and earned his Master of Science degree in Clinical Chemistry in 1982. While at Old Dominion University, Mr. Ayub held several Graduate Teaching Assistantships.

Mr. Ayub began study in the joint Old Dominion University and Eastern Virginia Medical School Biomedical Sciences Program in 1982. He recieved the Biomedical Sciences Program Fellowship for two terms. He advanced to the doctoral candidacy in March of 1987 and will recieve his doctorate from the Biomedical Sciences Program in 1988.